NATIONAL ADVISORY COMMITTEE FOR AERONAUTICS

TECHNICAL NOTE 3367

A DYNAMIC-MODEL STUDY OF THE EFFECT OF ADDED WEIGHTS AND OTHER STRUCTURAL VARIATIONS ON THE BLADE BENDING STRAINS OF AN EXPERIMENTAL TWO-BLADE JET-DRIVEN HELICOPTER IN HOVERING AND FORWARD FLIGHT

By John Locke McCarty and George W. Brooks

Langley Aeronautical Laboratory
Langley Field, Va.

Washington
May 1955

CONTENTS

NATIONAL ADVISORY COMMITTEE FOR AERONAUTICS

TECHNICAL NOTE 3367

A DYNAMIC-MODEL STUDY OF THE EFFECT OF ADDED WEIGHTS AND OTHER STRUCTURAL VARIATIONS ON THE BLADE BENDING STRAINS OF AN EXPERIMENTAL TWO-BLADE JET-DRIVEN HELICOPTER IN HOVERING AND FORWARD FLIGHT

By John Locke McCarty and George W. Brooks

SUMMARY

The blades of an experimental two-blade jet-driven helicopter are subject to a condition of near resonance between the frequencies of the first elastic bending mode of the blades and the third harmonic component of the aerodynamic loading which results in high bending strains during normal flight conditions. An experimental investigation has been conducted of a 1/10-scale dynamic model of the helicopter to determine the effect of various changes in the design configuration on the blade bending strains. These changes included the addition of different amounts of concentrated weight to the blades at various radial and chordwise locations and variations in the design counterweight locations, as well as changes in blade-pitch-control stiffness and blade bending stiffness. Tests were made under both hovering and forward-flight conditions up to a tip-speed ratio of approximately 0.18.

The results of the tests showed that the maximum bending strains occurred at tip-speed ratios in the vicinity of 0.10 and that the strains could be reduced materially by attaching to the blades, at proper radial stations, concentrated weights that would minimize the aforementioned condition of resonance. Further reductions in bending strains could be obtained by the proper location of the weight along the chord. A concentrated weight equal to 5 percent of the blade weight appeared to be about two-thirds as effective as a weight equal to 10 percent of the blade weight.

INTRODUCTION

The helicopter structure, by virtue of its mode of operation, is subjected to periodic loads having a wide range of frequencies. The externally applied aerodynamic forcing functions may be resolved into periodic components having frequencies equal to the various harmonics of

the rotational frequency of the rotor. In the conventional treatment of helicopter problems, the accepted assumptions of rotating-wing theory include the limitation that only the fundamental and very low harmonic components of the aerodynamic forcing function are significant. In recent years, experimental studies (for example, ref. 1) have shown that the magnitude of the rotor-blade bending moments due to the summation of the third through the tenth harmonic components may be as large as the combined contributions of the steady and the first two harmonic terms. Similar effects have been noted elsewhere and further references are listed in reference 1.

The large blade moments attributable to the higher harmonic inputs appear to exist primarily because the natural frequencies of certain blade bending modes are approximately equal to the frequencies of the harmonic loadings; thus conditions of resonance or near resonance are created. Experimental flight tests have also shown that large fuselage vibrations may exist if the natural frequencies of the fuselage are near the frequencies of the periodic components of the harmonic aerodynamic forcing function.

In 1949 the National Advisory Committee for Aeronautics constructed a 1/10-scale dynamic model of an experimental two-blade jet-driven helicopter with the primary objective of studying the flutter and ground-resonance characteristics under hovering conditions. During the course of this investigation, it was noted that a prominent 3-per-revolution blade bending oscillation occurred over a range of rotor speeds which included the design operating speed. A brief summary of the 3-per-revolution vibrations was presented, together with a description of the model and the results of the flutter and ground vibration studies in reference 2.

When the prototype full-scale helicopter was flown, the flight-test records showed that the 3-per-revolution blade bending vibrations previously found on the model under hovering conditions also existed on the prototype; furthermore, the flight tests showed that the amplitudes of the vibrations increased with forward speed to the extent that the blade bending stresses imposed severe limitations on the flight-test program. As suggested when the preliminary model test results were reported in reference 2, it appeared that the blade bending stresses were aggravated as a result of a condition of near resonance due to the proximity of the natural frequency of the first elastic bending mode of the blades to the third harmonic of the rotor speed.

In view of the critical nature of the blade-stress problem on this particular helicopter and the general interest on the subject of blade-stress amplification due to conditions of resonance, the NACA initiated a test program to evaluate means of reducing the blade stresses. The results of these tests, which were conducted on a 1/10-scale dynamic model

of the helicopter in the return passage of the Langley full-scale tunnel, are reported herein.

SYMBOLS

C_α	blade-pitch-control stiffness, ft-lb/radian
c	chord
f_{h_n}	frequency of nth elastic-bending-mode vibration, cpm
f_{α_n}	frequency of nth natural-torsion-mode vibration, cpm
m	mass of concentrated weight, slugs
M	total mass of blade, slugs
r	radial distance to blade element, ft
R	blade radius, ft
t	time, sec
V	tunnel speed, ft/sec
ϵ_n	strain of nth harmonic
μ	tip-speed ratio, $V \cos \alpha / R\Omega$ ($\cos \alpha$ assumed equal to 1, where α is the rotor angle of attack)
ϕ_n	phase angle of nth harmonic, deg (See section entitled "Method of Analysis and Presentation.")
Ω	rotor angular velocity, radians/sec

APPARATUS AND TEST PROCEDURE

Apparatus

The model test apparatus, consisting of the rotor and hub suspension system of a 1/10-scale dynamic model of a particular two-blade, jet-driven helicopter mounted on a tiltable support, is shown in figure 1. The

details of the rotor and suspension system are described in reference 2; however, for convenience, pertinent dimensions and features of the rotor and suspension system are given in the following sections, along with a description of the support mechanism and tunnel used in this investigation.

Rotor support.- The details of the rotor support, together with appropriate dimensions, are shown in figure 2. The upper portion of the mechanism can be tilted forward or backward through a range of $\pm 15^{\circ}$ by the electrically powered actuator. The model test apparatus was mounted on the floor in the return passage of the Langley full-scale tunnel with the center of the rotor located midway between the tunnel walls and 85.5 inches above the floor. The rotor support was designed to permit the pylon the same freedom of horizontal translation that it was afforded when attached to the model fuselage.

Rotor characteristics and configurations.- The two-blade rotor has a diameter of 13 feet and a solidity of 0.055. The blades are rectangular in plan form, are untwisted, have a chord of 6.8 inches, and have an NACA 23018 airfoil section. The blades are attached to the hub by means of blade-retention straps (fig. 3), which transfer the centrifugal forces to the hub and provide a flapping hinge at $r/R = 0.035$; no drag hinges are provided. The rotor is powered by a compressed-air pressure-jet system with four jet nozzles at each blade tip.

During the course of the investigation, tests were made for numerous changes to the blades and control system. Each change in the model is identified by a different configuration number. Altogether, 55 different configurations were tested. The configuration having a swash plate as the blade-pitch-control mechanism and an inboard and an outboard counterweight located 10.4 and 66.5 inches from the center of rotation, respectively, made up the basic configuration. The different configurations were obtained by (1) removal of the counterweights from the basic configuration, (2) relocation of and modifications to the outboard counterweight, (3) chordwise and radial location of different amounts of concentrated weight, (4) changes in the blade-pitch-control system, and (5) alterations to the blade bending stiffness.

The outboard counterweight was modified by the addition of 0.10 pound, or 2 percent of the blade weight, to the counterweight. The modifications are identified in tables I and II as modifications A and B. For modification A, the weight was located 22 percent of the chord forward of the blade leading edge whereas for modification B, the weight was located 55 percent of the chord forward of the leading edge.

Concentrated weights, in the form of lead strips, were also employed to evaluate the effects of changes in the radial and chordwise blade mass distributions on blade bending strains. These weights, weighing 1/4 pound

and 1/2 pound, provided mass ratios m/M of 0.05 and 0.10 (tables II and III). The concentrated weights were symmetrical about the blade chord and were held in position on the blade surface by means of industrial fiber-glass tape.

During most of the tests blade-pitch-control arms were coupled to a swash plate, which was preset before each group of tests to provide the desired collective and cyclic blade-pitch angles at the design rotor speed. However, as a means of varying the blade-pitch-control stiffness C_α to study the effect of blade-pitch-control stiffness on the blade bending strains, several tests were conducted with the blade-pitch control arms connected to a control beam mounted atop the pylon as shown in figure 3. By the proper selection of control-beam stiffness, the desired blade-pitch-control stiffness was obtained. Two control beams were used during the tests and, for purposes of identification, are referred to as control beam 1 and control beam 2. The blade-pitch-control stiffnesses for control beams 1 and 2 were 135 and 73 foot-pounds of applied torque per radian of rotation of the blade root, respectively. The effective control stiffness of the swash plate was 87.8 foot-pounds per radian. These variations are identified in tables I and II.

Further configurations were obtained by increasing the blade bending stiffness. (See table IV.) This additional stiffness was accomplished by gluing wood strips to the exterior surfaces of the blade and by fairing them so as to minimize any changes in the aerodynamic loadings.

The natural frequencies for several nonrotating blade configurations are listed in table V. The natural frequencies include those of the first two uncoupled elastic bending and torsion modes. These frequencies were experimentally obtained by exciting the blade, mounted on the support, in its various modes by means of an electromagnetic shaker. Although the numerous changes to the basic configuration had varying effects on the natural frequencies of the blades, the magnitudes of the changes are not believed to be sufficient to affect appreciably the mode shapes of the fundamental blade mode.

Tunnel characteristics.- The return passage of the Langley full-scale tunnel in the region of the model tests has a rectangular cross section (50 feet wide and 65 feet high). The mean velocity in the model test area could be varied up to a maximum of approximately 35 feet per second by varying the speed of the tunnel fans. A continuous record of the tunnel velocity was taken simultaneously with the records of blade strains and showed fluctuations in forward velocity of approximately ± 20 percent of the mean velocity. These fluctuations in velocity are shown in figure 4 where the boundaries of tunnel-velocity fluctuations are shown as a function of the mean tunnel velocity. The mean tunnel velocity is not defined as the average of the maximum and minimum values but represents

the tunnel velocity given by the visual mean of trace deflections on the oscillograph records. The records show that the random disturbances result in incremental decreases in velocity which are somewhat greater than the incremental increases. (See fig. 4.)

Instrumentation

The instrumentation of the rotor system consisted of an indicating tachometer, a 1-per-revolution rotor-speed timer, and strain-gage installations on the rotor. The outputs from the rotor-speed timer and the strain gages, together with that from the tunnel-velocity indicator, were recorded on oscillograph records. A section of a typical oscillograph record is shown in figure 5 for a tunnel velocity of 15 feet per second.

The indicating tachometer consisted of a small multipole generator, the armature of which was fixed to the rotor hub. The generator output was fed into a stroboscopic instrument.

The 1-per-revolution rotor-speed timer consisted of a spring-loaded brush-contactor arrangement which caused a break in an oscillograph galvanometer circuit once for each revolution of the rotor.

Electrical resistance strain gages were mounted on the surface of one blade on the quarter chord at stations 36, 46.6, and 57.6 to indicate blade bending and torsion deformations. Station numbers refer to the distance in inches from the center of rotation; the blade tip is station 78. Devices were also provided to indicate blade flapping motion and the motion of the pylon relative to the support, but these measurements were not used for the present analysis.

The wind-velocity measurements were obtained by means of a small sphere mounted on an instrumented cantilever beam. This sphere was mounted approximately in the plane of the rotor and was displaced horizontally from the center of the rotor a distance of 1 rotor radius forward and approximately 1 rotor diameter to the side.

Test Technique

All of the various model configurations, which were obtained as a result of one or more changes to the basic configuration (configuration 2) were tested under both hovering and forward-flight conditions. The testing technique involved increasing the rotor speed of the model to the normal or design value of 283 rpm, at which time the tunnel was brought up to the desired speed and an oscillograph record was taken of the rotor speed, tunnel velocity, and the strain-gage responses. This procedure was repeated for nine increments of tunnel velocity ranging

from 0 (model in hovering attitude) to the maximum value which corresponded to a tip-speed ratio μ of approximately 0.18. A continuous record was then taken as the tunnel velocity gradually decreased to 0 following the removal of the tunnel power.

Rotor-pitch and pylon-angle settings corresponding to normal flight conditions were frequently examined during the course of the tests to check for possible deviations. These angle settings included a collective-pitch setting of 5.8° with respect to the zero-lift line and a pylon tilt of 3.1° forward; for configurations employing the swash plate, there was a swash-plate tilt of 3.1° forward with respect to the direction of flow or 0° with respect to the shaft.

A few tests were also made at rotor speeds of 250, 300, and 350 rpm at various tunnel velocities; and, in some cases, continuous records were taken while the model rotor speed was varied from 283 to 350 rpm and the tunnel velocity was held constant.

METHOD OF ANALYSIS AND PRESENTATION

The procedure followed in the analysis of the data to obtain the blade bending strains may be described as follows. Simultaneous readings of the tunnel-velocity trace deflection and the double amplitudes of the envelope of the blade bending strain-gage trace deflections were measured at a number of points on the oscillograph records for each tunnel velocity. These trace deflections were then interpreted by means of calibration curves to obtain the tunnel velocity and blade bending strains. Calibration of the blade bending strains consisted of static tests which involved the application of known weights to the blade tip. The measured strains were then plotted as a function of tip-speed ratio as shown by the data presented for a typical configuration in figure 6. This figure shows the variation of blade bending strains with tip-speed ratio and illustrates that the strains are greatly increased as the tip-speed ratio is increased and reach a maximum in the transition region, $\mu \approx 0.10$. As further indicated by this typical case, the data for all configurations tested show a substantial variation in blade bending strains at a given tip-speed ratio. This apparent scatter of the data is possibly aggravated by the random turbulence of the flow through the rotor as a result of nonuniformity of the flow in the tunnel.

Because of the large number of configurations tested, it was essential to obtain a convenient method of summarizing the data to permit the various configurations to be readily compared on the basis of strains. Analysis of the data showed that a convenient way to obtain this summary would be to take an average of the measured strains for each configuration tested between certain limits of tip-speed ratio. In this respect, the

strains between μ of 0.06 and 0.16 were averaged to obtain a mean value for each configuration as shown by the straight line labeled "average" bending strain on figure 6. The values obtained for each configuration are listed in tables I to IV for three radial blade stations.

In addition to a comparison of the tabulated values of "average" strains, it is of interest to evaluate the effects of certain changes in the model configuration on blade bending strains throughout the range of tip-speed ratios achieved. For this purpose, curves were faired through the data points for the desired configurations in a manner similar to the way the curve is faired through the data points for the typical configuration shown in figure 6. The resulting curves, which show the effects of various changes in the model configuration, are presented and discussed in the section entitled "Results and Discussion."

The bending response of several blade configurations at station 36 was harmonically analyzed to determine the contribution of each of the first five harmonic components to the total periodic strain. This harmonic analysis made use of the following variation of strain with respect to time:

$$\epsilon(t) = \epsilon_1 \cos\left(\Omega t - \phi_1\right) + \epsilon_2 \cos\left(2\Omega t - \phi_2\right) + \epsilon_3 \cos\left(3\Omega t - \phi_3\right) + \epsilon_4 \cos\left(4\Omega t - \phi_4\right) + \epsilon_5 \cos\left(5\Omega t - \phi_5\right)$$

where $t = 0$ when the azimuth angle of the instrumented blade is approximately equal to 147° (the azimuth position of the instrumented blade when the timing blip is registered on the oscillograph record).

The harmonic analysis was obtained by dividing the azimuth angle during the course of one complete revolution of the rotor into 12 equal angles and measuring the strain-gage response obtained at each azimuth angle. This procedure was repeated for 10 successive revolutions of the rotor and the average value for each azimuth angle was computed. The average values were then used to calculate the various harmonic components and associated phase angles.

RESULTS AND DISCUSSION

Preliminary Studies

As pointed out in the introduction, during the initial tests (ref. 2) of this dynamic model, which were conducted to study its ground-resonance and flutter characteristics, it was observed that a prominent 3-per-revolution blade bending oscillation with resulting high strains was

encountered during hovering tests over a range of rotor speeds which included the design operating speed. The model test conditions under which these blade bending oscillations were observed and an indication of the relative amplitude of the associated strains were tabulated in reference 2. An analysis of these data led to the conclusion that these 3-per-revolution blade bending oscillations were possibly magnified by a condition of near resonance between the natural frequency of the first elastic bending mode of the blades and the third harmonic component of the aerodynamic loading on the blades. Results from flight tests of the prototype exhibited a similar condition of blade bending while hovering and, furthermore, indicated that the bending strains were magnified appreciably as the helicopter moved through the transition region from hovering to forward flight. In the latter case, the strains were of sufficient magnitude to impose severe limitations on the flight-test program of the helicopter.

The condition of resonance to which the amplification of the blade bending strain is attributed is shown by the frequency diagram of figure 7, where the uncoupled natural frequencies of the first elastic bending and torsion modes are plotted, together with harmonics of the rotor frequency as a function of the rotor speed. The natural frequencies of the nonrotating blade were measured experimentally, and the natural frequencies of the rotating blade were obtained by the application of calculated Southwell-type coefficients. (See ref. 3.) The frequency curve for the first torsion mode is presented here because it will be referred to later in a discussion of coupling of blade bending and torsion deformations due to chordwise displacement of added weights. An inspection of the relative frequencies at the normal operating rotor speed of 283 rpm shows the aforementioned condition of near resonance. In an effort to substantiate further the contention that the blade bending strains are amplified by conditions of resonance between the various harmonic lines and the frequency of the first elastic bending mode of the blade, additional studies of an exploratory nature were made under hovering conditions. These studies were made by operating the model at various rotor speeds up to and beyond the normal rotor speed and noting the rotor speeds where strain amplifications occurred. These rotor speeds are shown in figure 7 as the heavied portions of the various harmonic lines.

As was the case in the previous tests reported in reference 2, these results show predominant 3-per-revolution blade bending vibrations measured in the region of the normal operating rotor speed. Although the figure also shows a near-resonant condition at the normal operating speed between the frequencies of the first natural torsional mode and the fourth harmonic of the rotor speed, the predominant periodic strains measured on the blade were bending strains; this fact indicates that, for the basic blade configuration, the effect of this condition of near resonance between the fourth harmonic and the torsional frequency on the blade bending strains is negligible.

The most desirable step toward the elimination of objectionable resonance amplification of the blade strains would be to eliminate resonant conditions in the vicinity of the normal operating range of the helicopter. Since this may not be entirely feasible, it is then desirable to reduce the resonance amplification by separating the input and response frequencies to obtain acceptable strain levels. Because the third forcing harmonic line is fixed and the normal operating speed is determined from the consideration of performance, the permissible courses of action are:

(1) To change the curve of the natural bending frequency of the blade in order to minimize conditions of resonance

(2) To couple the blade bending and torsion deformations in such a manner as to provide effective aerodynamic damping.

One manner in which these objectives may be achieved is to attach concentrated weights to the blade at different radial and chordwise stations as discussed in the following paragraphs.

Figure 8 presents the results of an analytical study showing the effect on the model blade bending frequency of a 1/2-pound weight, which represents a mass ratio m/M of 0.10, located along the quarter-chord line at two blade radial stations. A weight added at the antinode of the first elastic bending mode of the blade would put the operating condition of the blades closer to a resonant condition at the normal operating rotor speed, and higher blade strains might be expected. In the same sense, the addition of weight at the nodal point would put the operating condition farther away from resonance with the third harmonic at the normal rotor speed and would suggest a reduction in the periodic blade bending strains.

Although the results of the preliminary studies indicated essentially no torsion strains, the frequency curves of figure 7 show that, at the normal operating rotor speed, the blade first elastic bending frequency is near that of the first torsion frequency. The proximity of these two frequencies would indicate the possibility of coupling of the blade bending and torsion modes for certain blade weight distributions.

In an effort to evaluate the extent to which the blade bending strains could be modified, as indicated by preliminary analyses, a number of configuration studies were conducted. The configurations tested as well as the results obtained are described in the sections that follow.

Effects of Variations in Flight Conditions

In order to permit a comparison of model and prototype test data, it was important to simulate the flight conditions involving pylon tilts,

cyclic and collective pitch angles, and rotor speeds of the prototype during the model tests. It was impractical, however, to maintain exact flight conditions. Fluctuations were present in the rotor speed because of small inaccuracies in the indicating tachometer and in the rotor attitudes because adjustments to the rotor did not readily permit angle settings to the exact desired values.

In general, the fluctuations in the angle settings and rotor speed could be maintained to within 5 percent of the mean value. However, it was of interest to determine to what extent these fluctuations would influence the blade bending strains and to evaluate the trends of variation of the blade bending strains which might result from large changes in pylon and swash-plate tilts and rotor speeds which might arise as a result of maneuvers and overspeed conditions. A discussion of the results of tests of this type is pertinent.

Effect of rotor speed.- The basic configuration (configuration 2) was studied both at the normal operating rotor speed of 283 rpm and at the condition of overspeed of 350 rpm. The results of these studies are given in figure 9, where the strains measured on the blade at the two rotor speeds are plotted as a function of the tip-speed ratio. The results indicate that small deviations in the rotor speed have little effect on the periodic blade bending strains, since operation of the basic configuration at overspeed yields strains that are roughly 10 percent greater than the strains measured at the normal rotor speed in the transition region. The strains resulting from operation of the model at overspeed in the hovering attitude, however, greatly exceeded those measured at the normal operating rotor speed.

Effect of variations in rotor attitudes.- A study of the effect of forward pylon tilt on the periodic strains was made on configuration 54 (table IV). This study was made by tilting the pylon, and consequently the entire rotor system, forward into the airstream with the swash plate remaining fixed with respect to the pylon. The results of this study are given in figure 10 where the periodic strains are plotted as a function of the tip-speed ratio. The pylon was tilted forward in intervals of 2° from the vertical to a maximum angle of 8°. From an overall consideration of the curves, forward pylon tilt has little effect on the maximum periodic bending strains within the range studied; however, for a pylon tilt of 0° the strains appear to be somewhat higher than those for the normal pylon setting of 3.1°. These data indicate that deviations of the pylon attitude from the desired setting of the order of magnitude encountered in the configuration studied would have little effect on the periodic blade bending strains except to change the variation of strains with respect to tip-speed ratio.

Changes in the swash-plate angle result in changes in the blade cyclic pitch angles with azimuth, or cyclic feathering, which, in turn,

lead to changes in the mechanical flapping of the rotor blades. Inasmuch as changes of a similar nature might occur under flight conditions involving maneuvers of various types, it was of interest to determine the extent to which such changes would influence the periodic blade bending strains. The periodic bending strains for five swash-plate tilt angles are shown as a function of tip-speed ratio in figure 11. The data indicate that changes in the swash-plate tilt settings of the order of magnitude encountered in effecting blade pitch settings would result in negligible changes in blade strain. However, the data show that the blade strains can be materially decreased by moving the swash plate from a rearward tilt of approximately 3° to a forward tilt of approximately 4°. Similar trends are shown by the blade bending strains for all three blade stations.

Effects of Variations in Blade Configuration

The results of the various configuration studies with respect to the effect of the changes itemized in tables I to IV on the periodic blade bending strains are discussed in the sections which follow.

Effect of removal of counterweights.- The counterweights were originally mounted on the blades to minimize the flutter problem; however, dynamic-model tests reported in reference 2 showed that the effect of counterweights on flutter was negligible. It was of interest then to determine whether or not removal of the counterweights would have any appreciable effect on the rotor-blade bending strains. For this reason separate tests were made on the blade with the inboard and outboard counterweights removed (configurations 13 and 16, table I). The results of these tests are presented in figure 12 where strains are compared with the strains of the basic configuration (configuration 2) and are plotted as a function of the tip-speed ratio for three radial stations.

The data indicate that, as compared with the basic configuration which has both counterweights attached, removal of the outboard counterweight increases the bending strains, whereas removal of the inboard counterweight decreases bending strains. Configurations other than the basic, however, show a less pronounced effect on the strains due to the elimination of each of the counterweights. Removal of the inboard counterweight, (for example, configuration 47, which had a concentrated weight added to the blade at station 62.5), resulted in little or no change in the bending strains, as is evident from comparison of the "average" bending strains of configurations 47 and 48. (See table III.)

Effect of outboard counterweight position.- In view of the fact that the preliminary studies indicated that a radial variation of the added weight influenced the blade strains and that there was a large amount of

weight already added to the blade in the form of counterweights, studies were made to determine whether the periodic bending strains could be reduced by a moderate radial movement of the outboard counterweight. The counterweight could not be moved outboard of its normal position at station 66.5 for structural reasons, so it was relocated at station 62.5. An example of the results of these studies is given in figure 13, wherein the strains of configurations 3 and 13 (table I) are compared over the test range of tip-speed ratios. The data show that the strains are increased by relocating the outboard counterweight from station 66.5 to station 62.5.

Effect of radial location of concentrated weight.- As discussed in the section entitled "Preliminary Studies," the results of the analytical calculations indicated that substantial changes in blade bending strains should result from the addition of concentrated weights along the quarter-chord line at different radial stations. These results were substantiated by data obtained for configurations 43 and 47 (table III) presented in figure 14(a). In addition, data are also presented in figure 14(b) for configurations 33 and 37 (table II), wherein concentrated weights were added to the leading edge of the blade. These figures show the variation in bending strain with tip-speed ratio at stations 36, 46.6, and 57.6. The strains measured for configuration 2, which had no concentrated weights, are also given in each case to permit a ready evaluation of the effects of the addition of the concentrated weights.

The trends shown by the data presented in both figures are similar insofar as the addition of concentrated weights to the blades definitely influences the periodic bending strains. The addition of weight to the blade at the antinode in each case results in strains which are considerably higher than the strains measured for the same blade configuration with no concentrated weights. Conversely, the addition of a concentrated weight at the nodal point results in a sizeable reduction in the blade strains. The aforementioned effects prevailed throughout the range of tip-speed ratios tested and resulted in the largest differences in blade strains at tip-speed ratios where the strains are approximately a maximum ($\mu = 0.10$).

Effect of chordwise location of concentrated weight.- As shown in figure 7 and pointed out in the section entitled "Preliminary Studies," the curves for the first natural bending and torsion frequencies of the uncoupled modes indicate that these frequencies at the normal rotor speed are approximately equal. Because of the nonuniform mass distribution of the blade, the possibility of coupling of blade bending and torsion deformation arises. For some of the configurations, particularly those involving the addition of concentrated weights at the nodal point in such a manner as to increase the bending frequency by tension effects and to reduce the torsion frequency by inertia effects, the natural frequencies of the bending and torsion modes would be closer to each other than for

the basic configuration (configuration 2) in figure 7. In view of the possible effects of coupling of the blade bending and torsion deformations on the periodic blade bending stresses, studies were made for various chordwise locations between the leading and trailing edges of the blade at stations 34 and 62.5. These studies were made to determine whether these modes could be coupled in such a manner as to reduce the periodic bending strains. The results of these tests are shown in figure 15(a) and 15(b), where the strains measured at stations 36, 46.6, and 57.6 are plotted as a function of the tip-speed ratio.

The data presented in figure 15(a) for concentrated weights added at the antinode (station 34) indicate that the blade strains are progressively decreased as the weight is moved from the leading to the trailing edge of the blade at stations 36 and 46.6 but not at station 57.6. The data presented for this station showed that slightly higher strains were obtained when the concentrated weight was mounted at the 60 percent chord than when the weight was mounted at the quarter chord. Conversely, the data presented in figure 15(b) for concentrated weights added at the nodal point (station 62.5) show that the strains are progressively increased as the weight is moved from the leading to the trailing edge of the blade. These trends prevail throughout the range of tip-speed ratios of the tests.

In an effort to afford a better comparison of the effect of chordwise location of concentrated weights at the aforementioned radial stations, the "average" values of the strains corresponding to each of the curves presented in figures 15(a) and 15(b), which are presented in table II, are plotted as a function of the chordwise location of the concentrated weight in figure 16. The method of obtaining the "average" strain from the measured data is discussed in the section entitled "Method of Analysis and Presentation." These strains are presented in terms of a strain ratio wherein the reference strain in each case corresponds to the "average" strain measured on the configuration with no concentrated weights. The data are presented for the three radial stations and, in each case, indicate that the addition of a concentrated weight at the antinode point results in strains which are higher than those for the configuration with no concentrated weights. The data further show that the addition of the concentrated weight at the nodal point at chordwise locations rearward of the approximate midchord appears to have essentially no effect on the bending strains. However, moving the concentrated weight toward the leading edge of the blade results in a reduction in the blade strains and suggests that the addition of the weight ahead of the leading edge at this spanwise station would yield a further reduction in the periodic blade bending strains.

Effect of mass ratio m/M.- In order to study the effect of mass ratio, tests were made wherein the amount of the concentrated weight added to the leading edge of the blade at station 62.5 was varied. The

results of these tests are presented in figure 17, where the strain is again plotted as a function of the tip-speed ratio for three values of the mass ratio m/M. The data show that the reduction in the periodic blade bending strains with the addition of concentrated weight is apparently nonlinear. The reduction in the bending strains for the addition of a concentrated weight equal to 5 percent blade weight is approximately two-thirds of the reduction obtained for the addition of a concentrated weight equal to 10 percent of the blade weight.

Effect of blade-pitch-control stiffness.- The effect of changes in the blade-pitch-control stiffness C_α is to change the frequencies of the natural torsion modes f_α of the blades (table V). Since the proximity of bending and torsion frequencies at the design rotor speed suggests the possibility of coupling between blade bending and torsion deformations, it was of interest to determine the effect of changes in the blade torsional frequency on the blade bending strains. Tests were made for different blade-mass configurations during which the blade-pitch-control stiffness was varied by use of control beams 1 and 2 (C_α = 135 and 73 foot-pounds/radian, respectively.) The results of those tests are presented in figure 18, where the strains measured at stations 36, 46.6, and 57.6 are plotted as a function of tip-speed ratio for each configuration.

The data presented in figure 19 show that the strains are increased by an increase in blade-pitch-control stiffness C_α, both for the case having no concentrated weights added to the blade and for the case with 5 percent blade weight added at station 34 at 60 percent chord. However, the data show that the effect of increasing the blade-pitch-control stiffness is slightly beneficial when 5 percent of the blade weight is added at station 62.5 at the blade leading edge.

The results show that the change in coupling brought about by variations in the chordwise location of the concentrated weight is much more effective in changing the bending strains than that brought about by variations in the torsional control stiffness.

Effect of increasing blade bending stiffness.- An analysis of the relationship between the first natural bending frequency of the blade and the frequency of the third harmonic component of the aerodynamic loading (fig. 7) suggested that an increase in the blade bending frequency would be beneficial from the standpoint of minimizing the effects of resonance amplification. Tests conducted wherein the blade natural frequencies were increased by changes in blade mass distribution upheld this contention and led to an exploratory study of the effect of increasing the natural frequency by increasing the bending stiffness of the blade between stations 43 and 64. The results of these studies are presented in

figure 19, where the blade strains measured at stations 36, 46.6 and 57.6 are given as a function of tip-speed ratio for three blade configurations.

These data indicate that the major effect of stiffening the outboard section of the blades is to change the radial distribution of blade strains. The strains measured at station 36 show that an increase in blade stiffness in the manner described results in a substantial increase in the bending strain, probably due to stress concentration near the ends of the strips. The data presented further show that the effect on the blade strains measured at station 46.6 is negligible, whereas the effect on the blade strains measured at station 57.6 appears inconsistent.

Harmonic Analysis

A comparison of the strains measured during the course of this investigation shows that the amplitudes of the strains vary considerably as a result of changes in the model configuration. Inasmuch as changes in configuration cause variations in the natural bending and torsion frequencies of the blades, there are resulting changes in the relationships between the natural frequencies of the rotor blades and the various harmonics of the rotational frequency. A harmonic analysis of the strain records of a few representative configurations was made, therefore, to obtain an idea of the harmonic content. In this regard, 12-point analyses were made to determine the amplitudes and corresponding phase angles of the first five harmonic components for configurations 2, 3, 13, 43, 47, and 48. The results of these analyses are given in table VI for the bending response at station 36. These configurations were selected because of the desire for a more detailed study of the effect of the radial location of a concentrated weight (configurations 2, 43, and 47), the effect of outboard counterweight location (configurations 3 and 13), and the effect of the inboard counterweight (configurations 47 and 48). The data presented in figure 20 for the basic configuration (configuration 2) illustrate that the information in table VI can be plotted to obtain the variations in the harmonic components of strain and the corresponding phase angles with the tip-speed ratio.

An example of the manner in which the amplitudes of the various components vary for changes in configurations is shown in figure 21. The strain resulting from each harmonic component at a tip-speed ratio of 0.08 is plotted in the form of a bar graph for three configurations involving different radial locations of a concentrated weight. These graphs are obtained by reading the strain of each harmonic component at a selected tip-speed ratio of 0.08 from curves such as the one presented in figure 20 where the data for the basic configuration were obtained. It was concluded from the analytical studies that the addition of a concentrated weight at the antinode of the blade would put the natural frequency of the blades closer to resonance with the third harmonic of the rotor frequency at the

normal operating speed and would result in increased strains over the basic configuration. Similarly, according to the analytical studies, the addition of a concentrated weight at the blade nodal point would reduce the effects of resonance so that the periodic blade strains are decreased. These conditions are substantiated by the amplitude of the third harmonic component of the strains shown in figure 21.

Results of these and the other configurations harmonically analyzed can be plotted in a similar fashion for other tip-speed ratios.

CONCLUSIONS

The results of a systematic study of the effects of various changes in the design configuration of the blades of a 1/10-scale dynamic model of an experimental two-blade jet-driven helicopter suggest the following conclusions with regard to blade bending strains:

1. The bending strains encountered during simulated forward-flight conditions were substantially greater than those encountered during hovering conditions. The tip-speed ratio was varied from 0 to approximately 0.18 for each model configuration studied; and, in nearly all cases, the maximum bending strains were measured at a tip-speed ratio of approximately 0.10.

2. The blade bending strains showed that the maximum bending moment occurred in the vicinity of radial station 46.6, that is, 46.6 inches from the center of rotation.

3. Amplifications of the bending strain were noted when a condition of resonance or near resonance existed between the frequency of the blade in its first elastic bending mode and the frequencies of the harmonic loadings. The third harmonic loading was of primary interest because a resonant condition between this harmonic and the natural bending frequency existed near the normal operating rotor speed of 283 rpm.

4. The addition of a concentrated weight to the blade on the quarter chord at the radial location of the antinodal point of the first natural bending mode aggravated the condition of resonance and increased the blade bending strains. The addition of a concentrated weight at the nodal point minimized the condition of resonance and resulted in a reduction in the blade bending strains. This reduction appeared reasonable when the effect of concentrated weights on the blade bending frequency was analyzed.

5. The addition of a concentrated weight equal to 5 percent of the blade weight appeared to be about two-thirds as effective in changing the blade strains as a weight equal to 10 percent of the blade weight.

6. Variation in the chordwise location of the concentrated weights affected the coupling of the bending and torsional blade deformations and resulted in substantial changes in blade bending strains. The lowest blade bending strains were obtained when the concentrated weight was located at the leading edge of the blade at the radial location of the node of the first elastic bending mode.

7. Changes in the first torsional frequency of the blade of ±10 percent obtained by variation of the blade-pitch-control stiffness resulted in only minor changes in the blade bending strains.

Langley Aeronautical Laboratory,
National Advisory Committee for Aeronautics,
Langley Field, Va., November 12, 1954.

REFERENCES

1. Daughaday, H., and Kline, J.: An Approach to the Determination of Higher Harmonic Rotor Blade Stresses. Proc. Ninth Annual Forum, Am. Helicopter Soc., Inc., May 14-17, 1953, pp. 90-126.

2. Brooks, George W., and Sylvester, Maurice A.: Description and Investigation of a Dynamic Model of the XH-17 Two-Blade Jet-Driven Helicopter. NACA RM L50I21, 1951.

3. Den Hartog, J. P.: Mechanical Vibrations. Third ed., McGraw-Hill Book Co., Inc., 1947.

TABLE I

MODEL CONFIGURATIONS AND RESULTS WITH NO CONCENTRATED WEIGHT ADDED TO BLADE

Configuration	Pitch-control mechanism	Inboard counterweight	Outboard counterweight stations, in.	Outboard counterweight modification	"Average" bending strain		
					Station 36	Station 46.6	Station 57.6
1	Swash plate	On	66.5	None	287×10^{-6}	----------	----------
2	Swash plate	On	66.5	None	311	432×10^{-6}	404×10^{-6}
3	Swash plate	Off	62.5	None	278	411	412
4	Control beam 1	Off	62.5	None	320	470	428
5	Control beam 2	Off	62.5	None	337	447	430
6	Swash plate	Off	62.5	A	224	325	321
7	Control beam 1	Off	62.5	A	284	378	347
8	Control beam 2	Off	62.5	A	280	371	346
9	Swash plate	Off	62.5	B	208	312	314
10	Control beam 2	Off	62.5	B	230	310	294
11	Control beam 1	Off	62.5	B	262	342	320
12	Swash plate	Off	66.5	None	254	350	329
13	Swash plate	Off	66.5	None	259	326	287
14	Swash plate	Off	66.5	B	166	271	----------
15	Swash plate	Off	66.5	B	173	276	272
16	Swash plate	On	None	None	374	561	499
17	Swash plate	Off	62.5	B	197	318	284

TABLE II

MODEL CONFIGURATIONS AND RESULTS WITH 1/4-POUND CONCENTRATED WEIGHT ADDED TO BLADE (m/M = 0.05)

Configuration	Pitch-control mechanism	Inboard counterweight	Outboard counterweight stations, in.	Outboard counterweight modification	Chordwise location of concentrated weight, percent chord		"Average" bending strain		
					Station 34	Station 62.5	Station 36	Station 46.6	Station 57.6
18	Swash plate	Off	62.5	A	60	---	319×10^{-6}	456×10^{-6}	394×10^{-6}
19	Control beam 2	Off	62.5	B	60	---	303	428	381
20	Control beam 1	Off	62.5	B	60	---	374	476	392
21	Control beam 1	Off	66.5	A	60	0	271	348	324
22	Control beam 2	Off	66.5	A	60	0	312	355	339
23	Swash plate	Off	62.5	None	91	---	312	480	486
24	Swash plate	Off	62.5	A	91	---	267	398	365
25	Swash plate	Off	66.5	None	100	0	238	347	314
26	Swash plate	Off	Off	None	100	100	320	519	499
27	Swash plate	On	66.5	None	---	0	207	565	----------
28	Control beam 1	Off	66.5	A	---	0	193	301	295
29	Control beam 1	Off	66.5	B	---	0	192	280	275
30	Control beam 2	Off	66.5	B	---	0	199	266	276
31	Control beam 2	Off	66.5	A	---	0	212	301	304
32	Swash plate	Off	66.5	B	0	---	265	364	----------
33	Swash plate	Off	66.5	B	0	---	263	357	311
34	Swash plate	Off	66.5	B	25	---	248	355	294
35	Swash plate	Off	66.5	B	60	---	214	342	313
36	Swash plate	Off	66.5	B	100	---	187	306	277
37	Swash plate	Off	66.5	B	---	0	138	205	217
38	Swash plate	Off	66.5	B	---	25	152	250	245
39	Swash plate	Off	66.5	B	---	60	174	272	284
40	Swash plate	Off	66.5	B	---	100	173	283	279
41	Swash plate	Off	62.5	B	60	---	241	399	349

TABLE III

MODEL CONFIGURATIONS AND RESULTS WITH 1/2-POUND CONCENTRATED WEIGHT ADDED TO BLADE (m/M = 0.10)

[Pitch-control mechanism - swash plate]

Configuration	Inboard counterweight	Outboard counterweight stations, in.	Chordwise location of concentrated weight, percent chord		"Average" bending strain		
			Station 34	Station 62.5	Station 36	Station 46.6	Station 57.6
42	On	66.5	0	--	526×10^{-6}	----------	----------
43	On	66.5	25	--	495	647×10^{-6}	534×10^{-6}
44	On	Off	25	--	516	670	553
45	On	66.5	--	0	148	----------	----------
46	On	66.5	--	25	199	----------	----------
47	On	66.5	--	25	209	297	271
48	Off	66.5	--	25	188	263	266
49	On	66.5	--	25	176	263	288
50	On	66.5	25	--	425	----------	----------

TABLE IV

ADDITIONAL MODEL CONFIGURATIONS AND RESULTS

[Pitch-control mechanism - swash plate]

Configuration	Inboard counterweight	Outboard counterweight stations, in.	"Average" bending strain			Remarks
			Station 36	Station 46.6	Station 57.6	
51	Off	66.5	181×10^{-6}	267×10^{-6}	----------	Concentrated weight of 0.12 pound added to blade leading edge at station 75.
52	Off	66.5	277	303	312×10^{-6}	Blade bending stiffness increased approximately 25 percent between stations 43 and 64.
53	Off	66.5	387	309	254	Blade bending stiffness increased approximately 50 percent between stations 43 and 64.
54	On	66.5	----------	----------	----------	Variation in pylon tilt - swash plate fixed with respect to pylon.
55	On	66.5	----------	----------	----------	Variation in swash-plate tilt - normal pylon position maintained.

TABLE V

NONROTATING NATURAL FREQUENCIES OF VARIOUS BLADE CONFIGURATIONS

Configuration	Frequency, cpm			
	f_{h_1}	f_{h_2}	f_{α_1}	f_{α_2}
2	511.8	1746	960	1920
3	503.4	1680	1095	2448
4	521.4	1686	1338	2724
5	513	1680	900	2349
7	-----	----	1122	2400
11	-----	----	987	2358
12 and 13	480	1716	1212	2598
52	517.8	1800	1032	2400
53	540	1842	1050	2346

TABLE VI

TABULATION OF RESULTS OF HARMONIC ANALYSES OF BLADE BENDING RESPONSE AT STATION 36

$$\left[\epsilon(t) = \epsilon_1 \cos\left(\Omega t - \phi_1\right) + \epsilon_2 \cos\left(2\Omega t - \phi_2\right) + \epsilon_3 \cos\left(3\Omega t - \phi_3\right) + \epsilon_4 \cos\left(4\Omega t - \phi_4\right) + \epsilon_5 \cos\left(5\Omega t - \phi_5\right)\right]$$

Configuration	μ	First harmonic		Second harmonic		Third harmonic		Fourth harmonic		Fifth harmonic	
		ϵ_1	ϕ_1	ϵ_2	ϕ_2	ϵ_3	ϕ_3	ϵ_4	ϕ_4	ϵ_5	ϕ_5
2	0.047	119.6×10^{-6}	230.3	25.2×10^{-6}	125.3	91.8×10^{-6}	184.3	18.2×10^{-6}	138.8	10.4×10^{-6}	31.0
	.065	116.1	240.0	65.8	161.5	169.0	205.3	11.3	118.6	9.5	217.9
	.132	78.0	237.2	71.9	114.1	164.6	169.1	2.6	180.0	23.4	197.1
	.150	49.4	265.0	53.7	107.9	143.9	175.1	38.1	193.1	34.7	151.5
3	.036	130.0	229.1	16.5	22.4	67.6	168.1	19.9	105.3	2.6	198.4
	.105	106.6	237.6	96.2	83.8	100.5	138.5	30.3	126.9	15.6	189.5
	.104	91.0	249.3	66.7	100.4	91.8	131.2	7.8	192.5	9.5	195.3
	.145	49.4	281.1	76.2	80.2	49.4	185.0	13.9	195.0	27.7	188.9
13	.047	105.8	251.9	57.2	136.8	123.0	219.3	24.2	243.8	5.2	288.4
	.086	86.7	256.7	52.0	144.5	128.2	224.2	6.0	351.5	9.5	221.2
	.122	68.4	241.2	76.2	144.7	171.7	198.9	23.2	182.1	19.1	223.2
	.162	34.7	275.7	57.2	96.9	62.4	190.4	25.9	160.5	4.3	201.8
43	.056	132.6	244.4	91.9	134.2	226.0	236.3	18.2	225.0	11.3	26.6
	.091	124.0	232.5	109.2	145.1	398.0	250.0	19.1	236.3	22.5	183.5
	.126	82.3	230.1	99.7	135.4	359.5	235.3	16.5	132.9	7.8	200.6
	.153	59.8	271.7	83.2	120.1	185.5	192.7	9.5	206.6	26.9	183.7
47	.018	96.1	233.4	36.4	114.1	52.0	185.7	12.1	144.0	5.2	141.4
	.079	83.1	220.3	42.4	101.8	67.5	150.8	5.2	149.0	11.3	193.0
	.110	64.1	222.8	37.3	108.9	44.2	161.6	13.9	150.3	22.7	193.5
	.163	33.8	226.1	23.4	126.0	30.3	140.8	16.5	137.1	21.7	163.7
48	.033	78.0	236.3	5.2	149.0	29.4	186.7	5.2	108.4	5.2	189.5
	.088	79.7	226.8	29.5	106.9	67.6	140.2	7.8	49.4	19.9	195.3
	.125	53.7	238.9	42.5	100.6	52.0	156.5	14.7	100.0	28.6	180.0
	.161	32.0	279.2	39.9	85.0	44.2	147.9	16.5	71.6	21.6	191.3

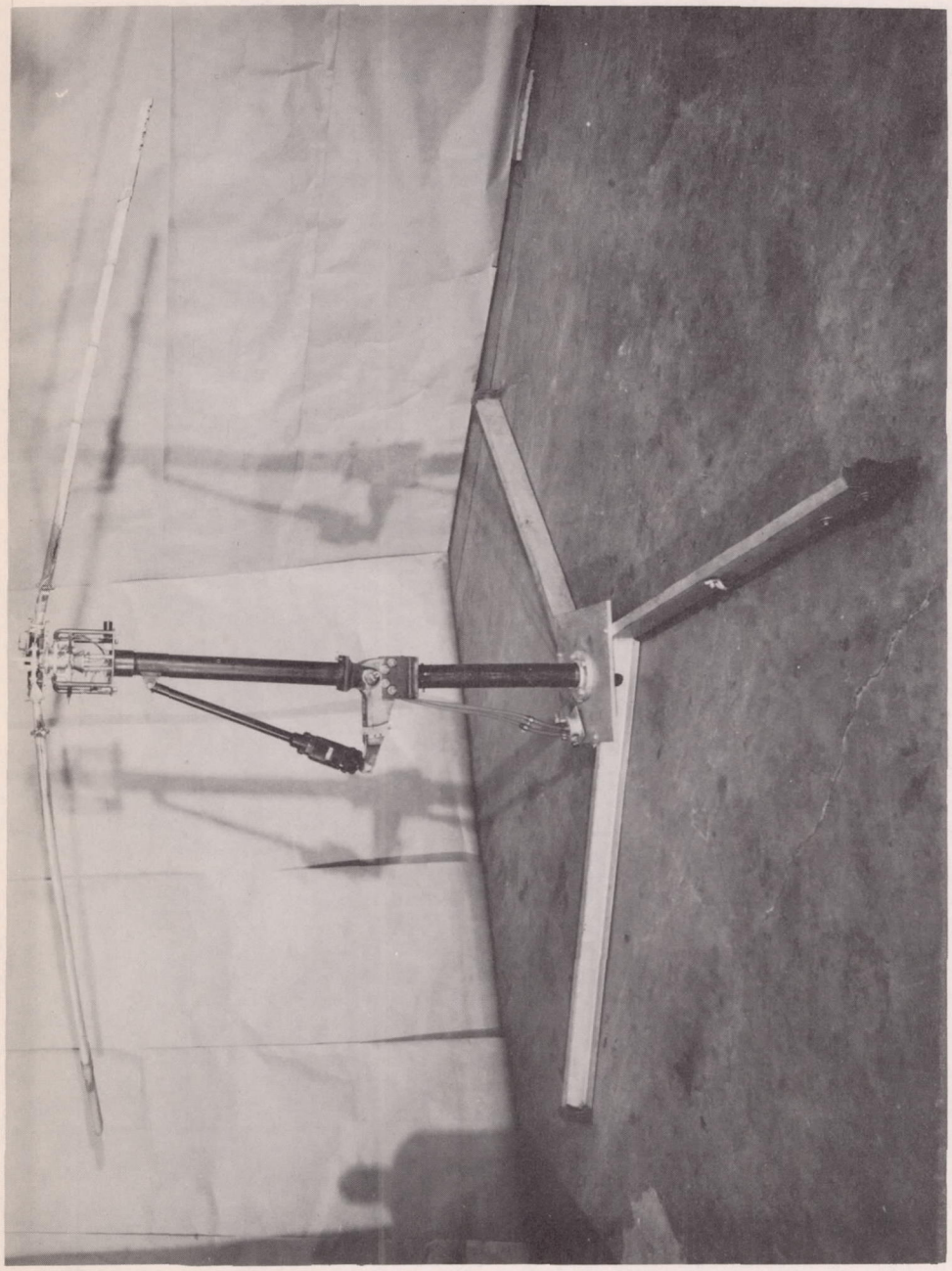

L-85028

Figure 1.- Model test apparatus.

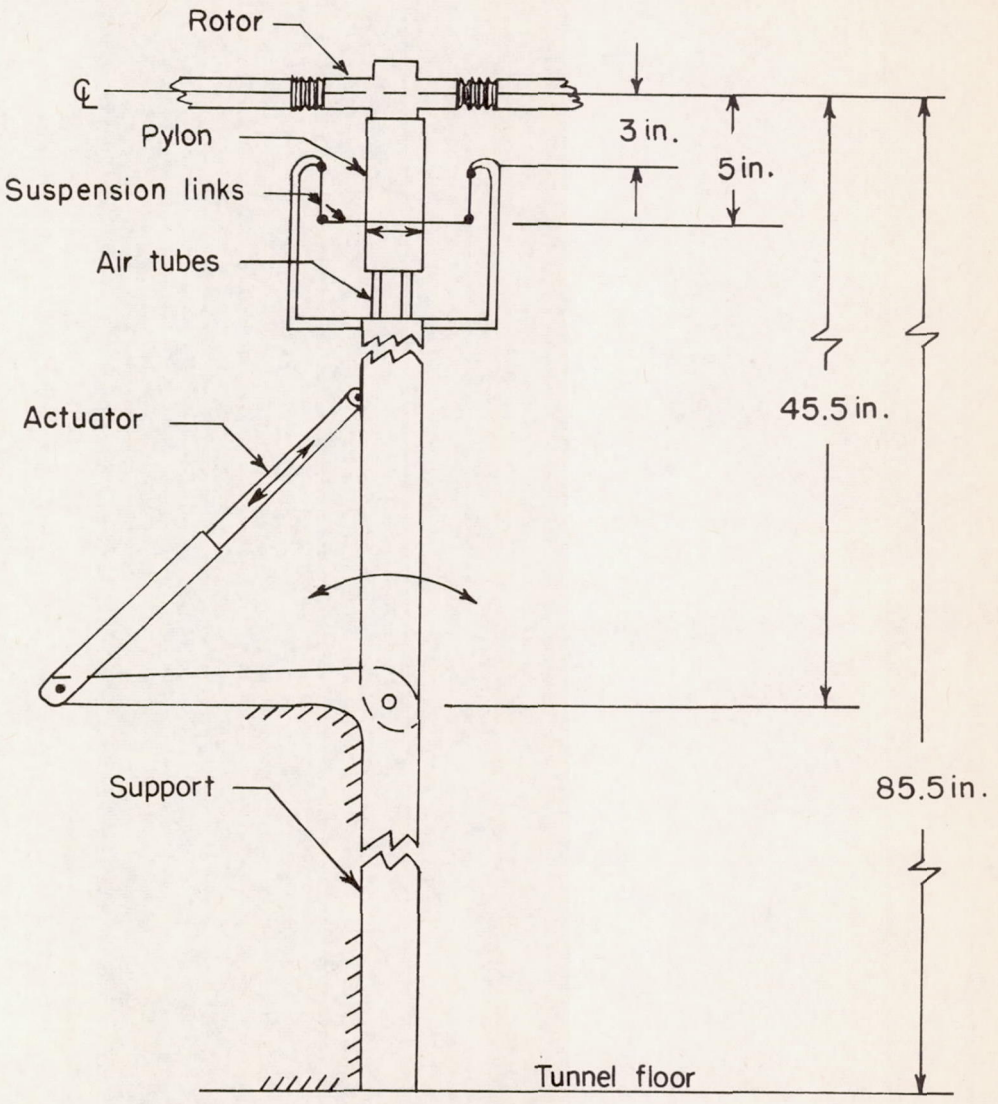

Figure 2.- Dimensional sketch of rotor support.

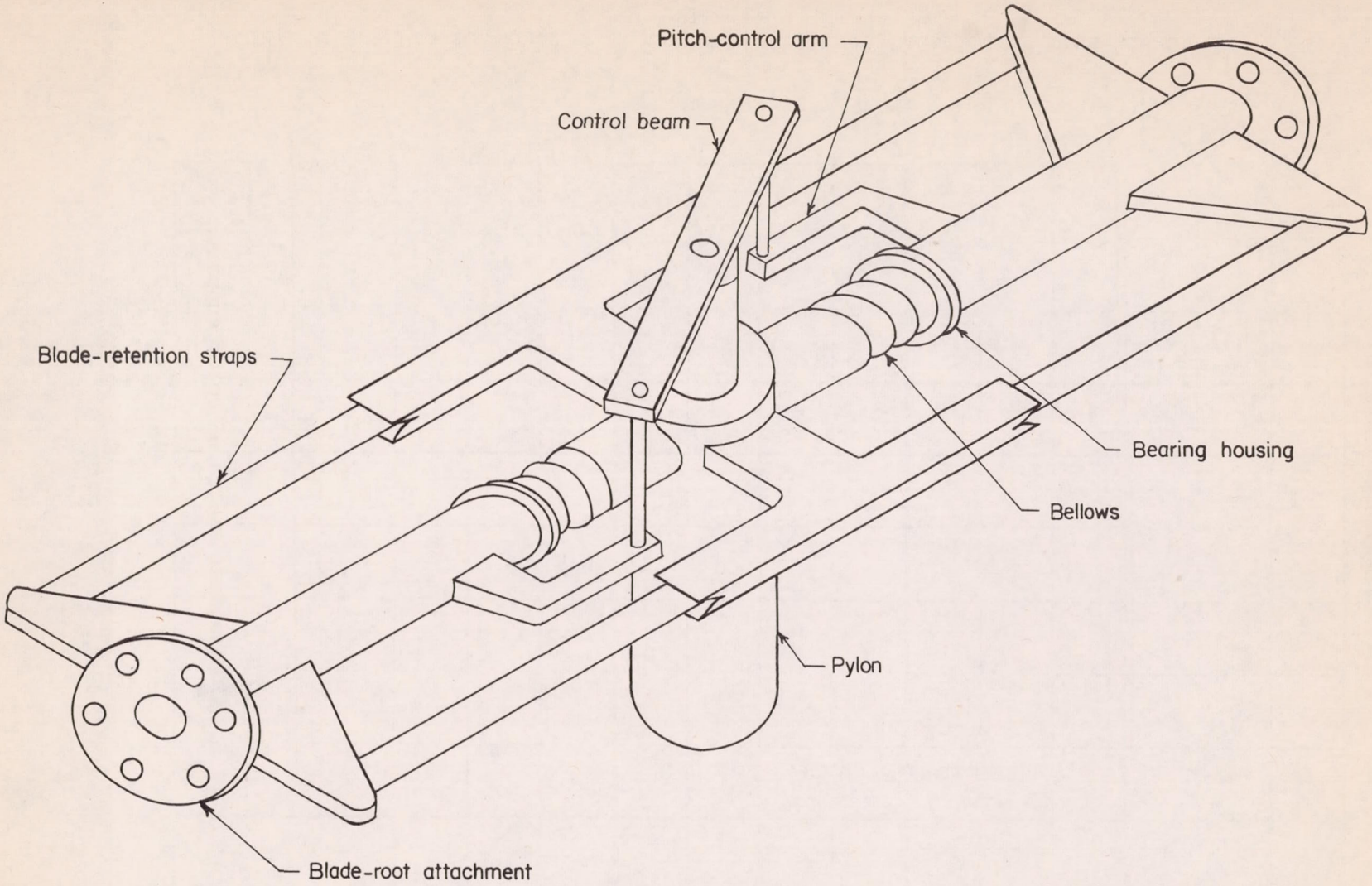

Figure 3.- Schematic drawing of rotor hub showing control-beam installation.

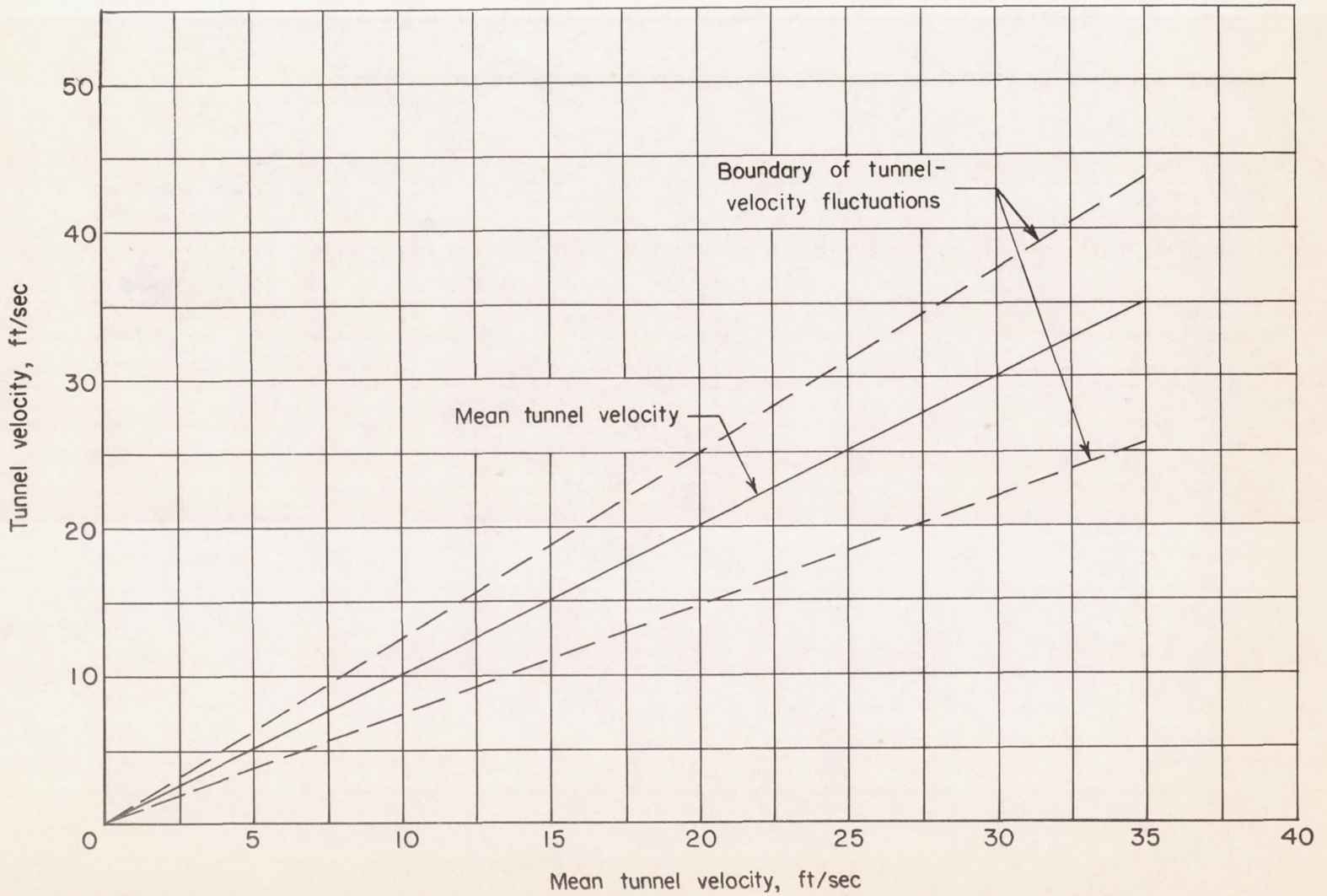

Figure 4.- Fluctuations in tunnel velocity as a function of mean tunnel velocity.

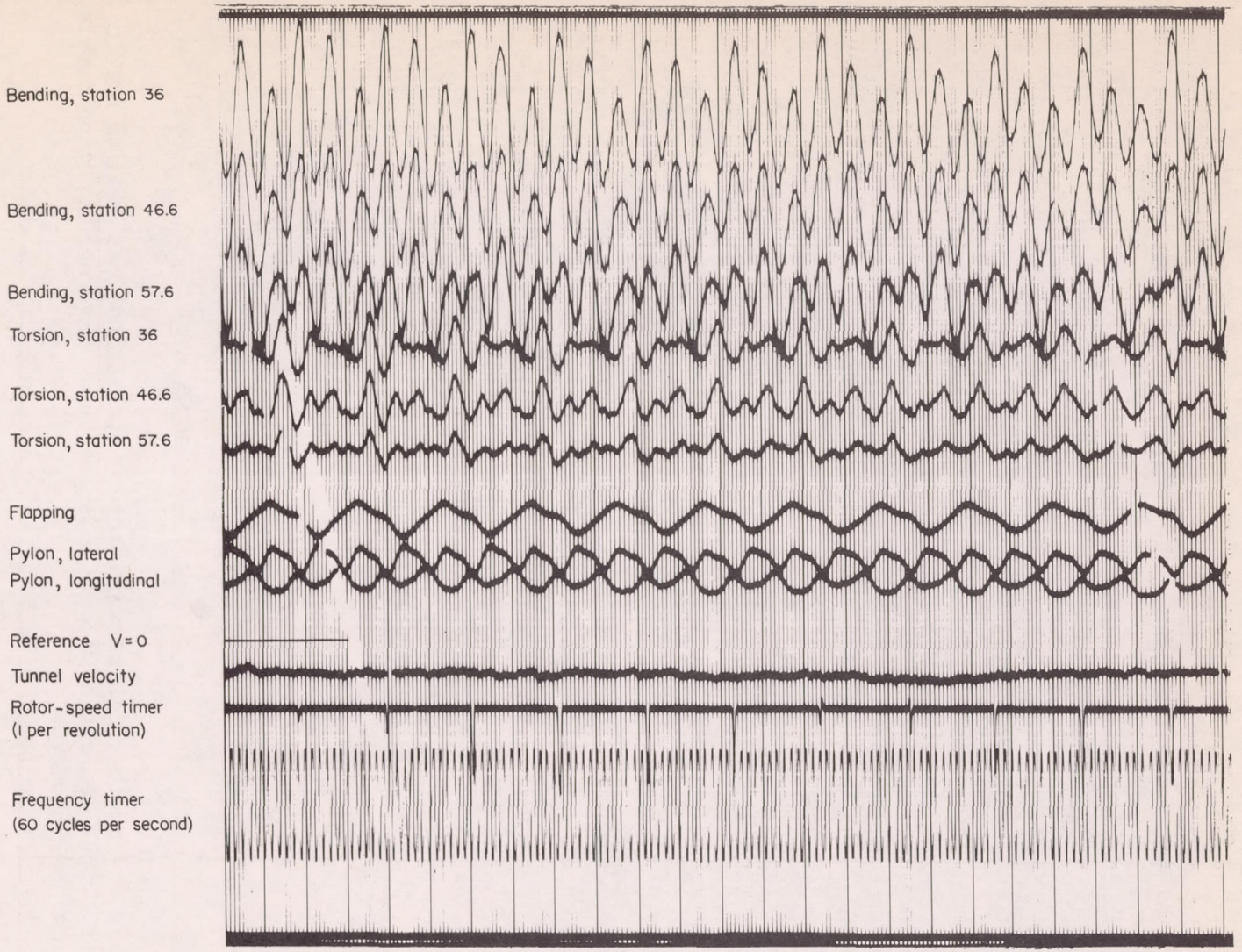

Figure 5.- Section of typical oscillograph record. V = 15 ft/sec.

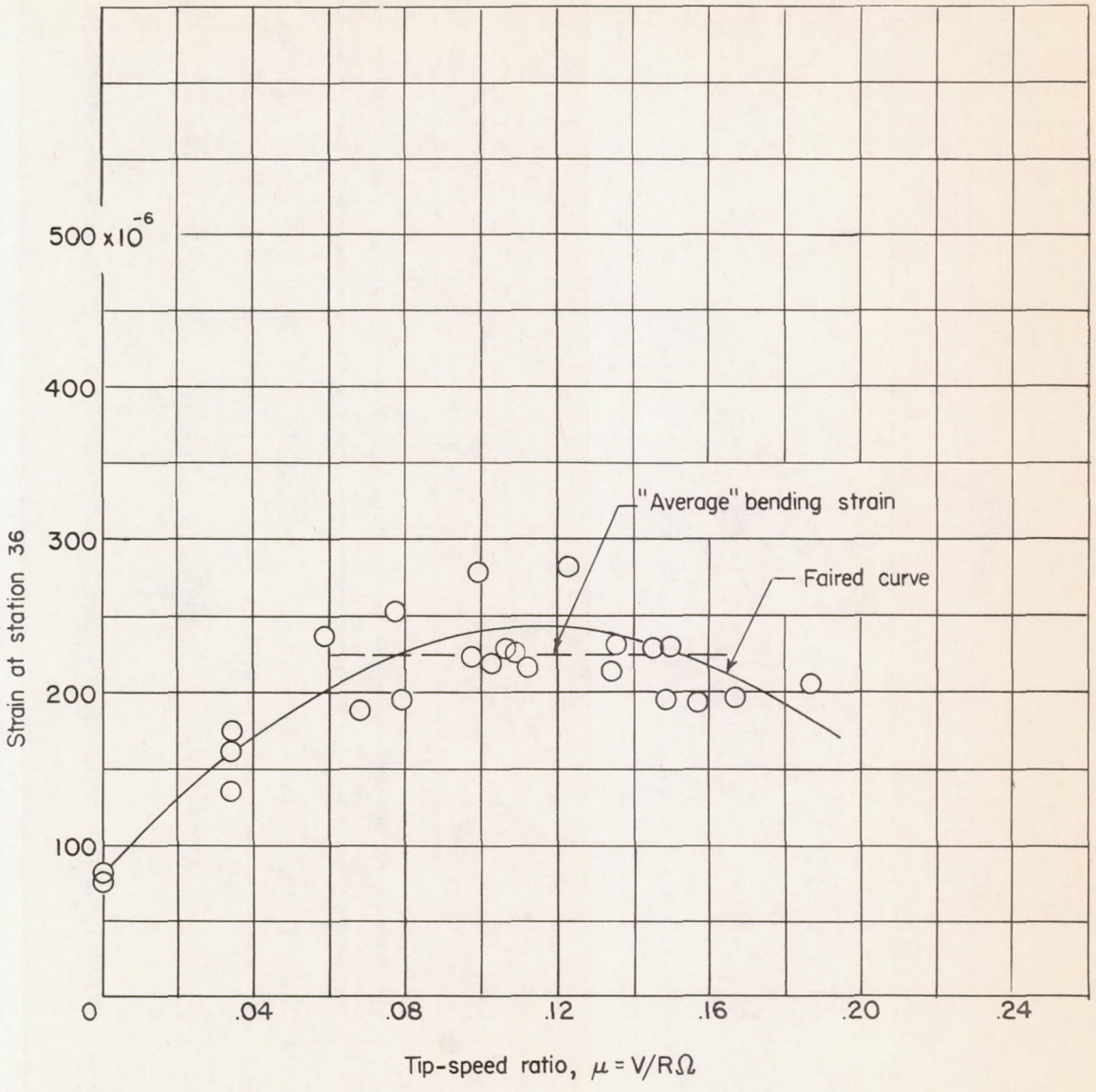

Figure 6.- Typical relationship between periodic blade bending strain and tip-speed ratio showing measured data, "average" bending strain, and faired curve.

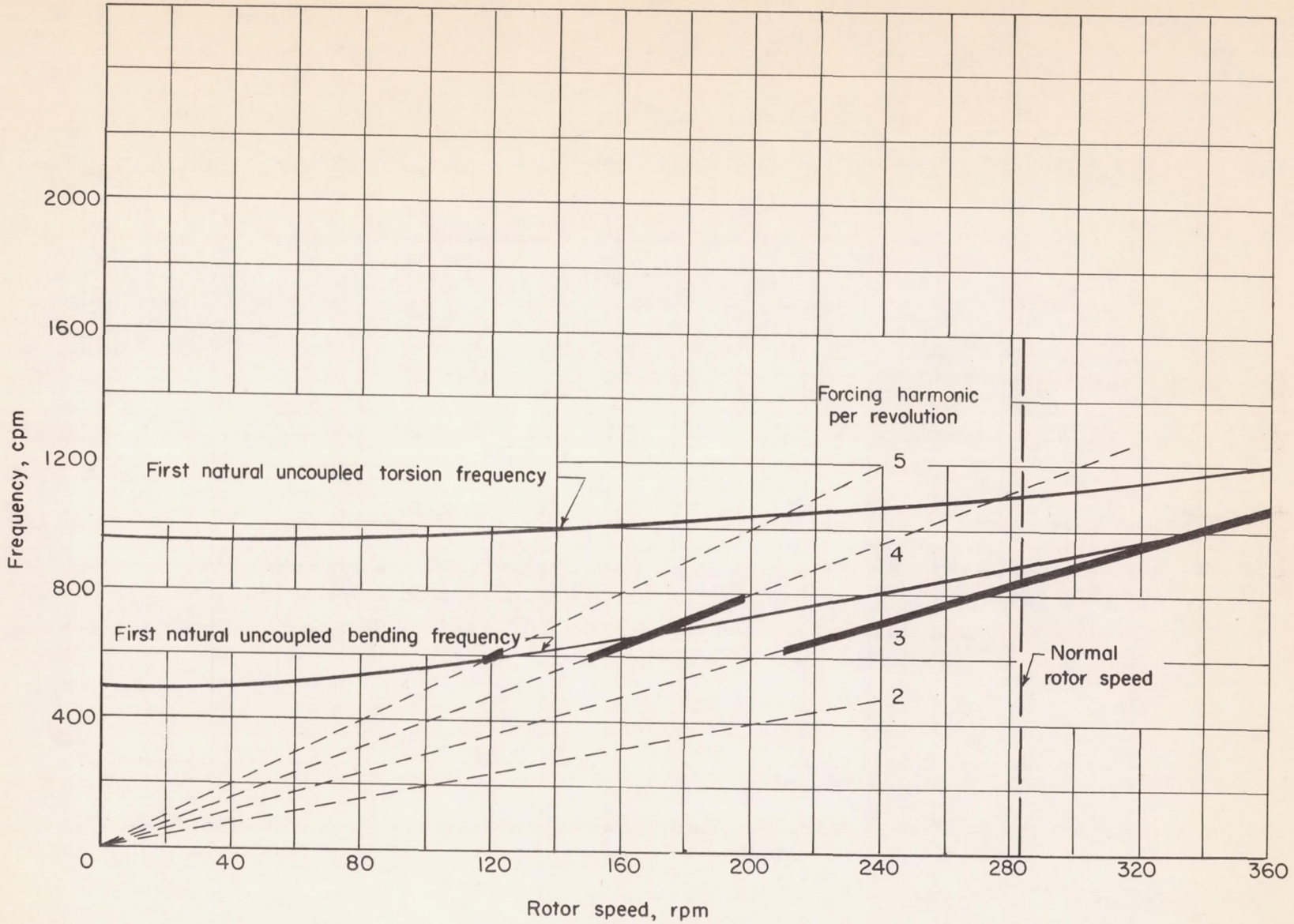

Figure 7.- The natural and resonant blade frequencies of basic configuration.

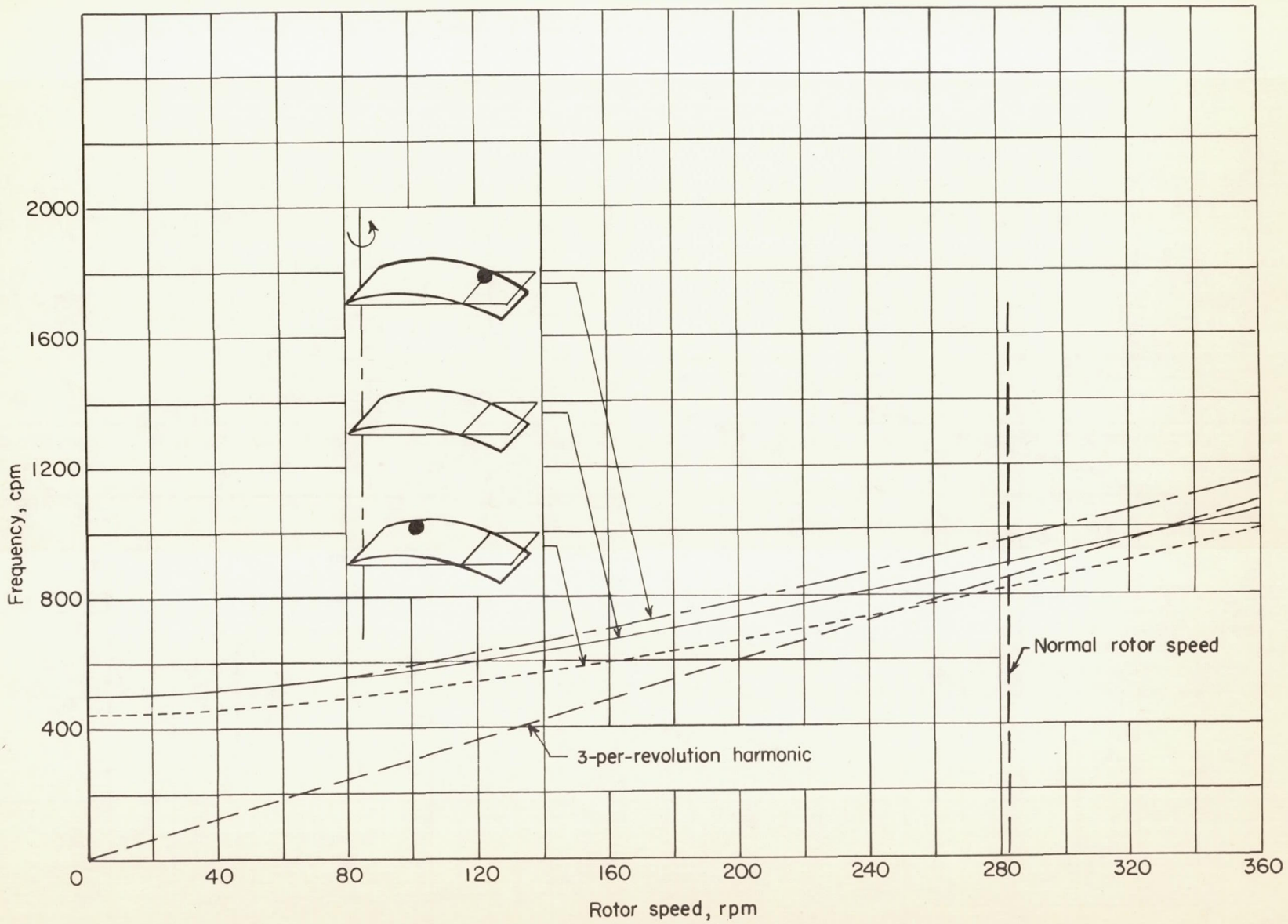

Figure 8.- Effect of concentrated weights on first natural uncoupled blade bending frequency. m/M = 0.10.

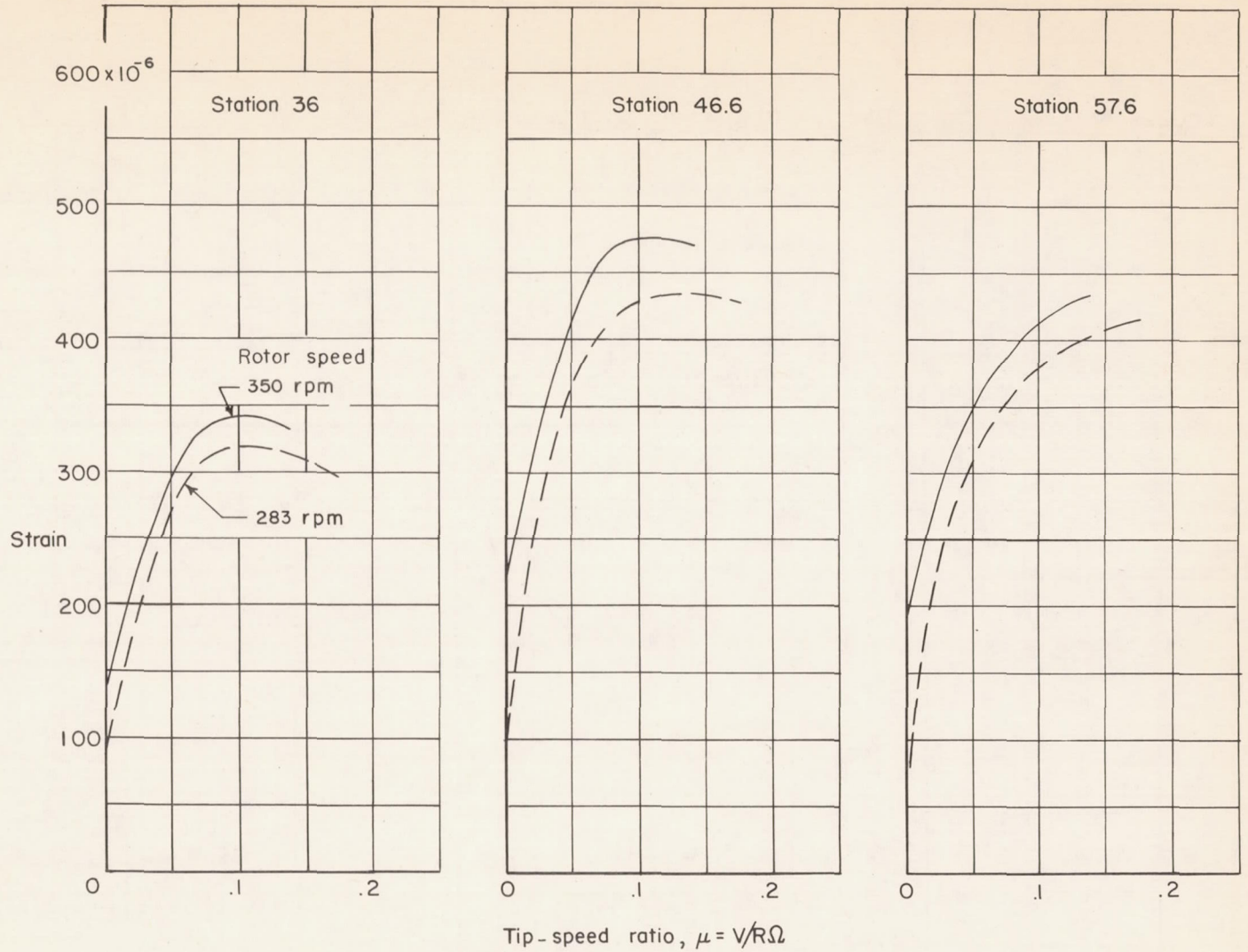

Figure 9.- Effect of rotor speed on periodic blade bending strains. (Basic configuration, configuration 2.)

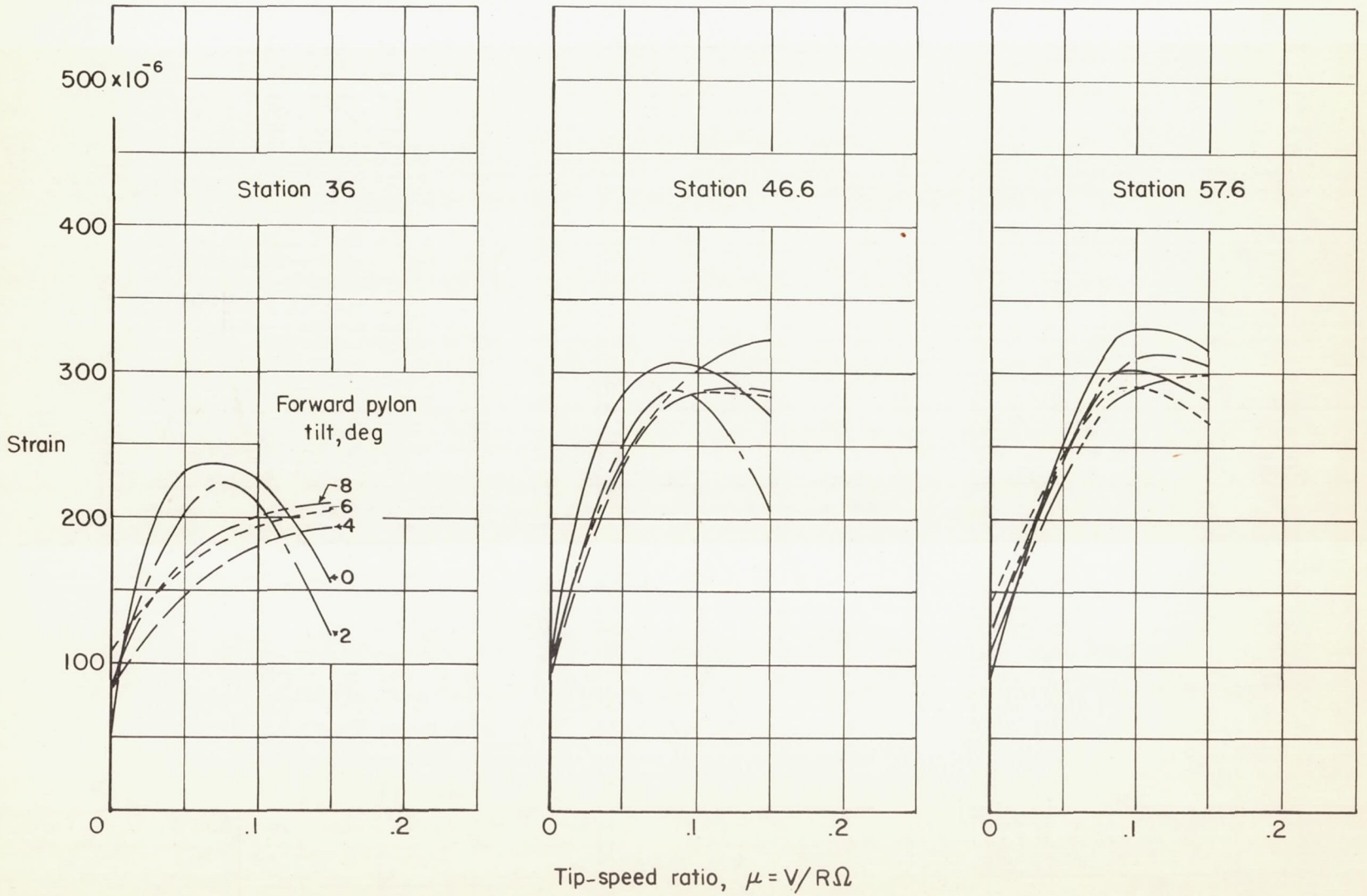

Figure 10.- Effect of forward pylon tilt on periodic blade bending strains. (Configuration 54.)

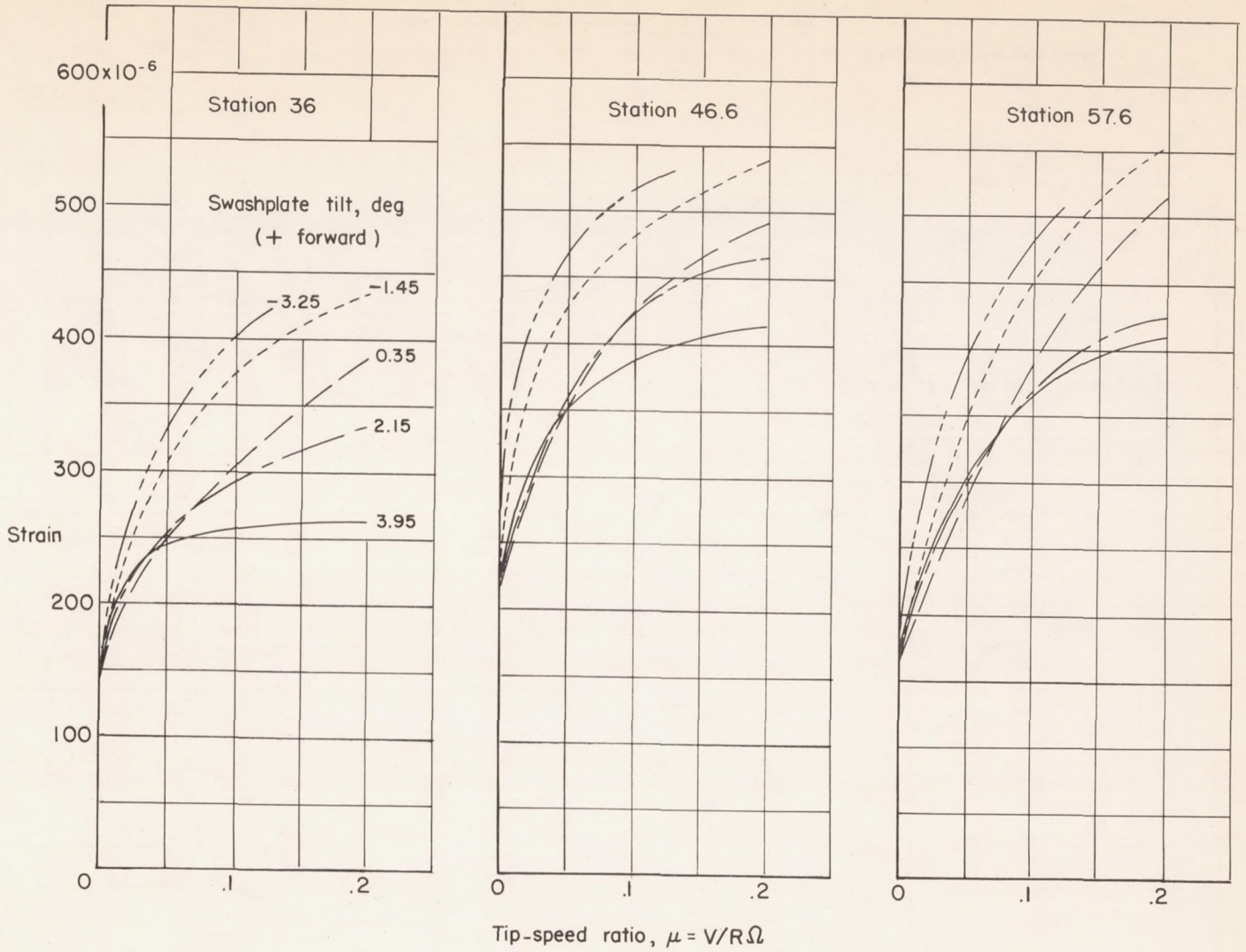

Figure 11.- Effect of swash-plate tilt on periodic blade bending strains. (Configuration 55.)

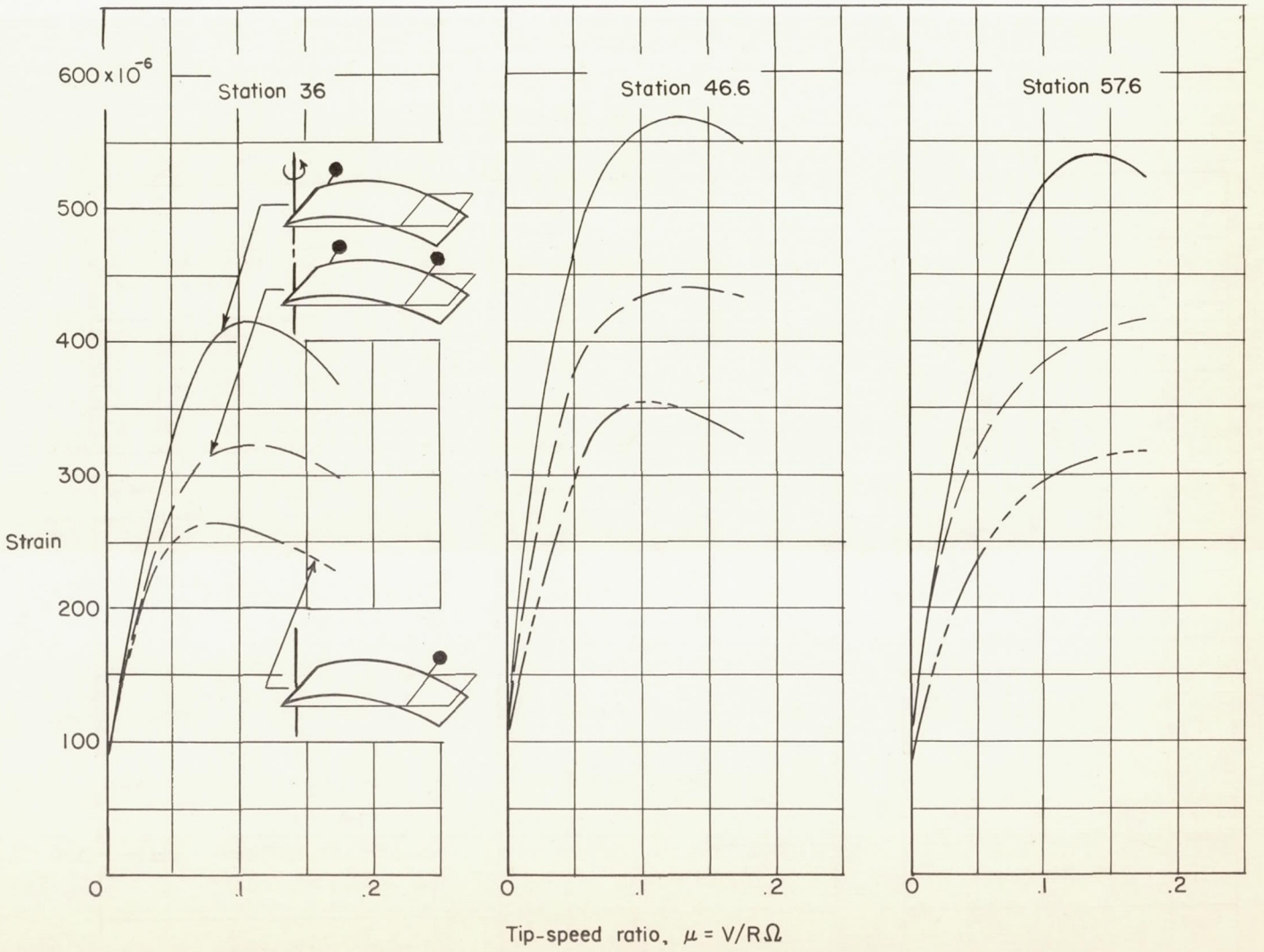

Figure 12.- Effect of design counterweights on periodic blade bending strains. (Configurations 2, 13, and 16.)

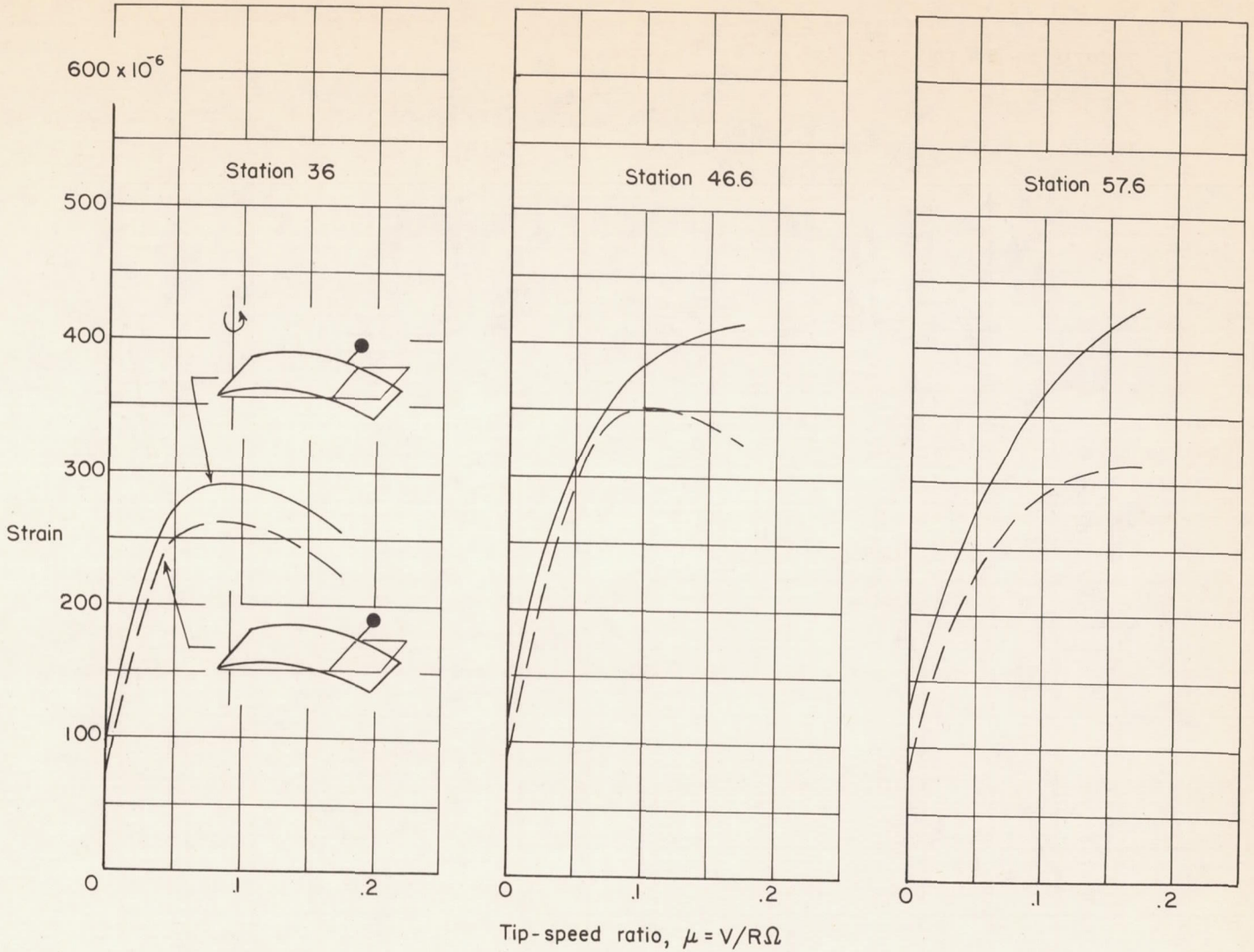

Figure 13.- Effect of outboard counterweight position on periodic blade bending strains. (Configurations 3 and 13.)

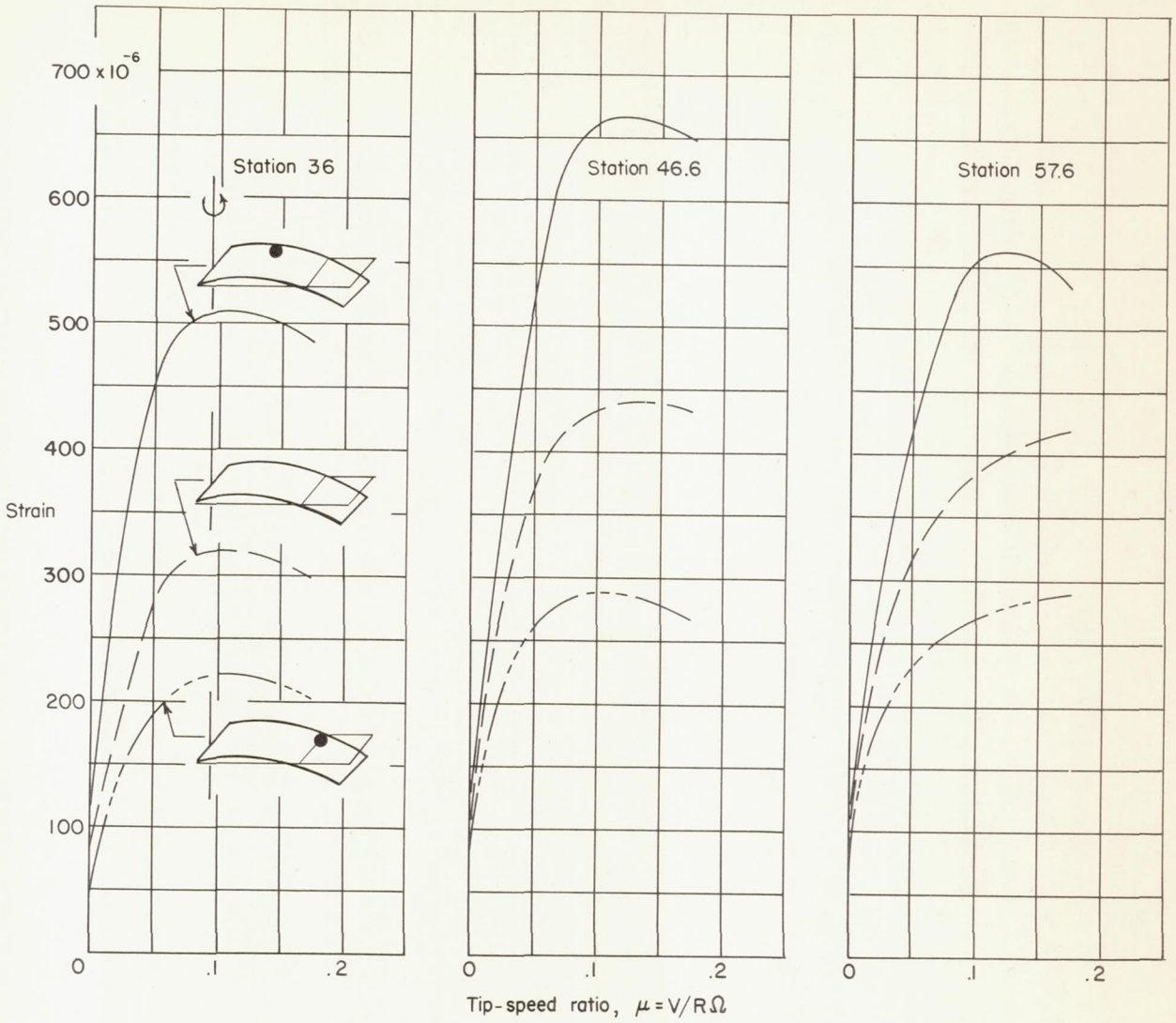

(a) Configurations 2, 43, and 47; m/M = 0.1 at blade quarter chord.

Figure 14.- Effect of radial location of concentrated weight on periodic blade bending strains.

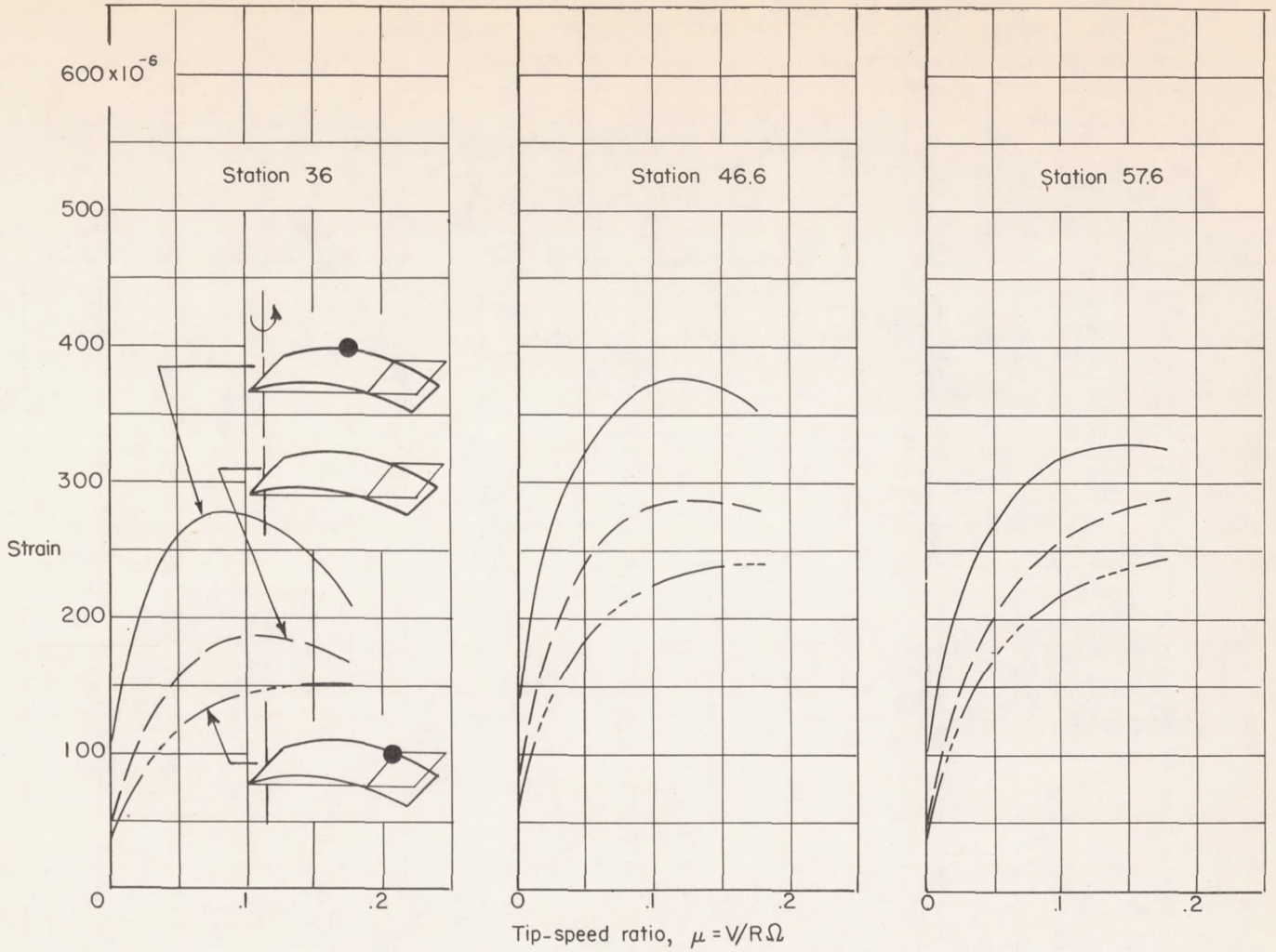

(b) Configurations 15, 33, and 37; m/M = 0.05 at blade leading edge.

Figure 14.- Concluded.

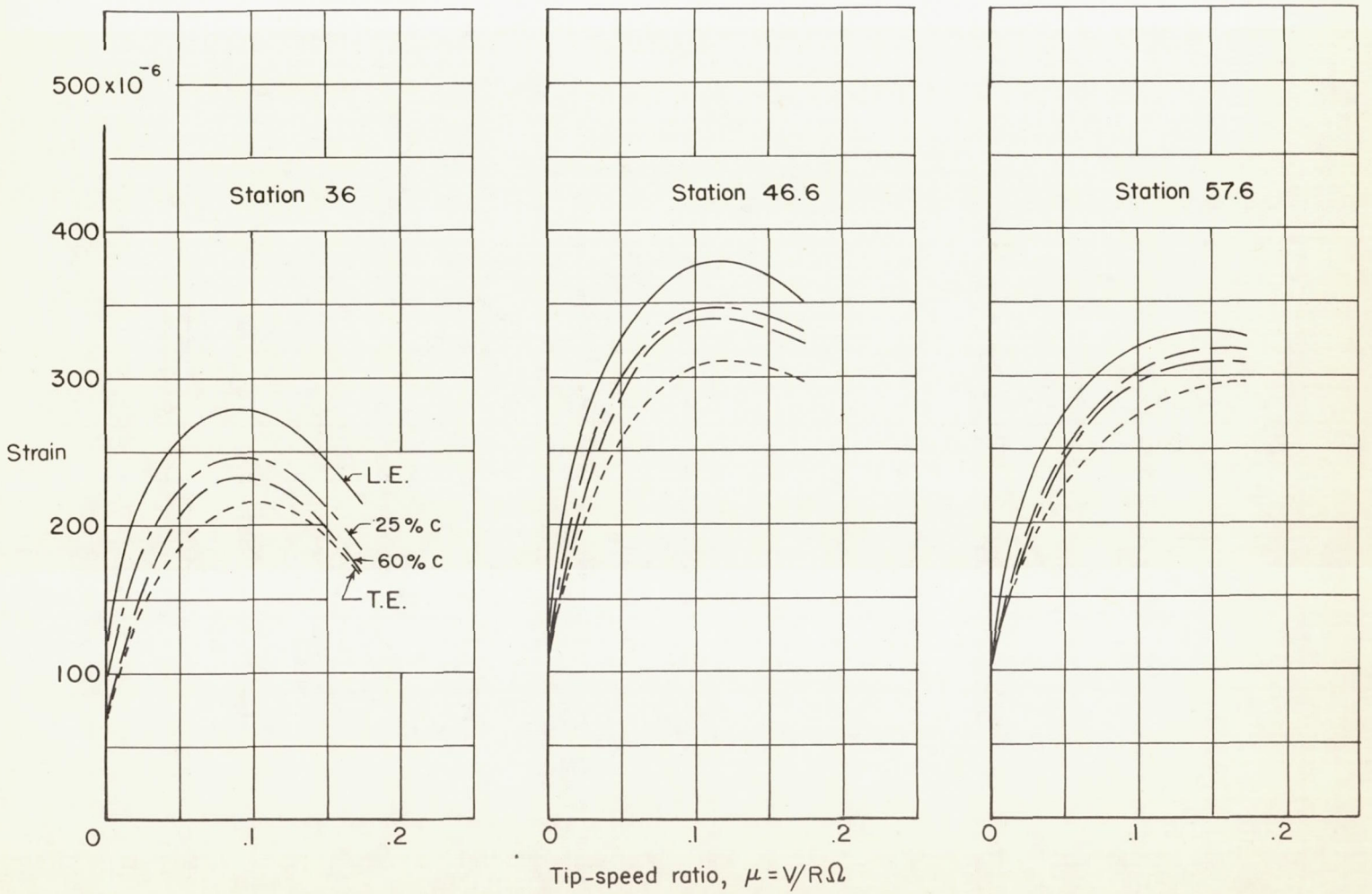

(a) Configurations 33, 34, 35, and 36; m/M = 0.05 at station 34.

Figure 15.- Effect of chordwise location of concentrated weight on periodic blade bending strains.

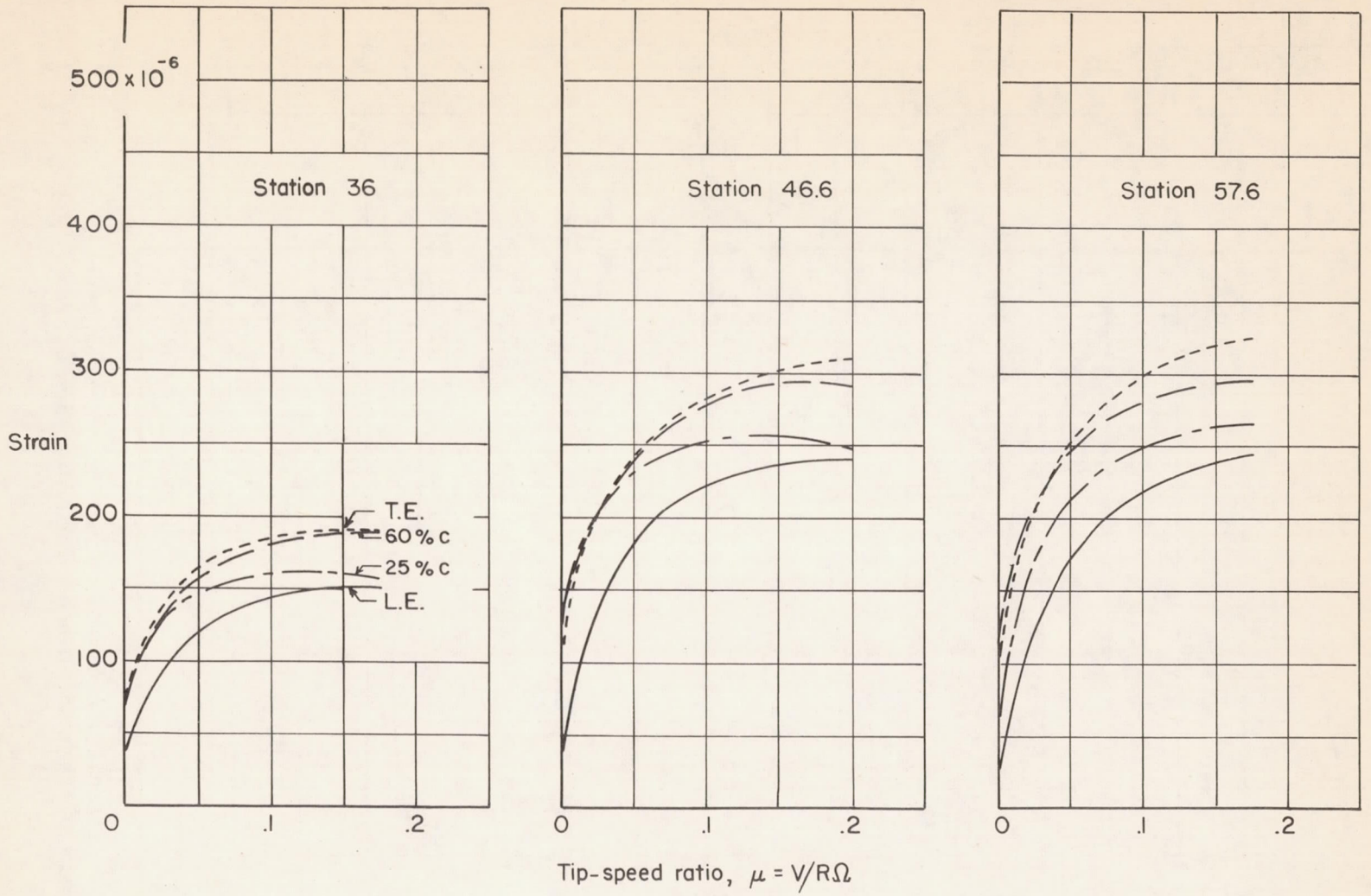

(b) Configurations 37, 38, 39, and 40; m/M = 0.05 at station 62.5.

Figure 15.- Concluded.

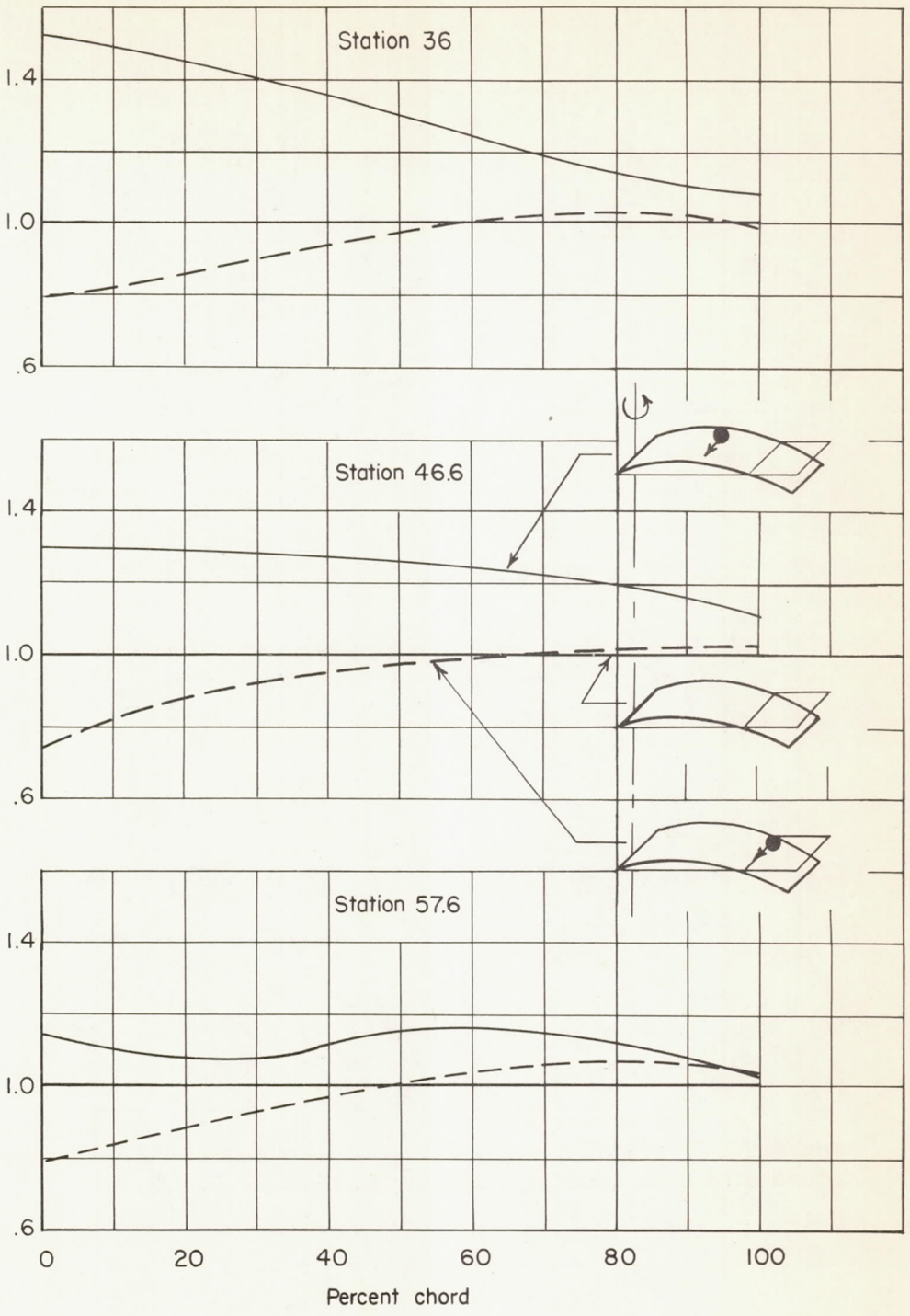

Figure 16.- Effect of chordwise location of concentrated weight on "average" periodic blade bending strains. m/M = 0.05.

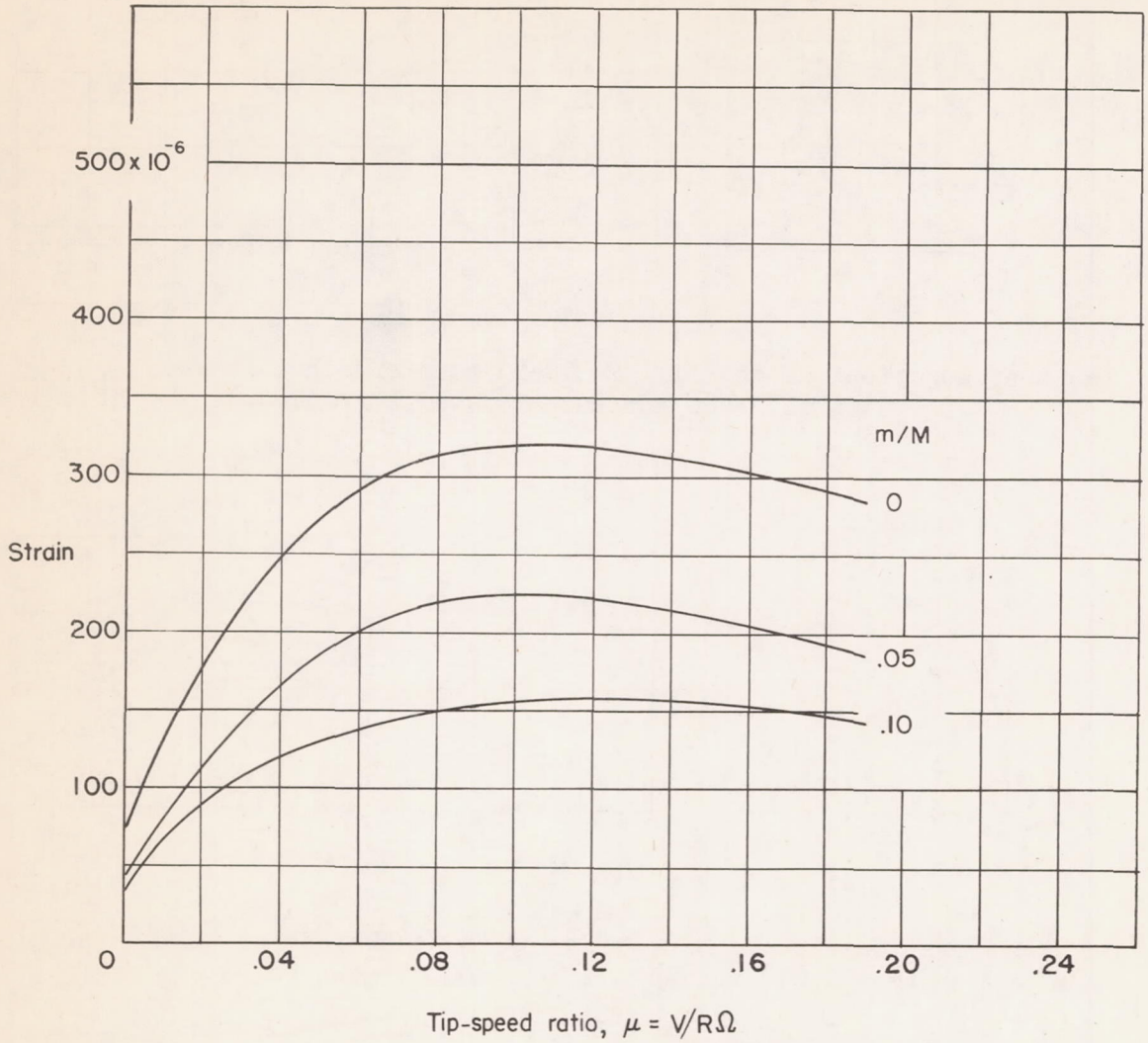

Figure 17.- Effect of mass ratio m/M on periodic blade bending strains measured at station 36. Configuration numbers 2, 27, and 45. Mass added to blade leading edge at station 62.5.

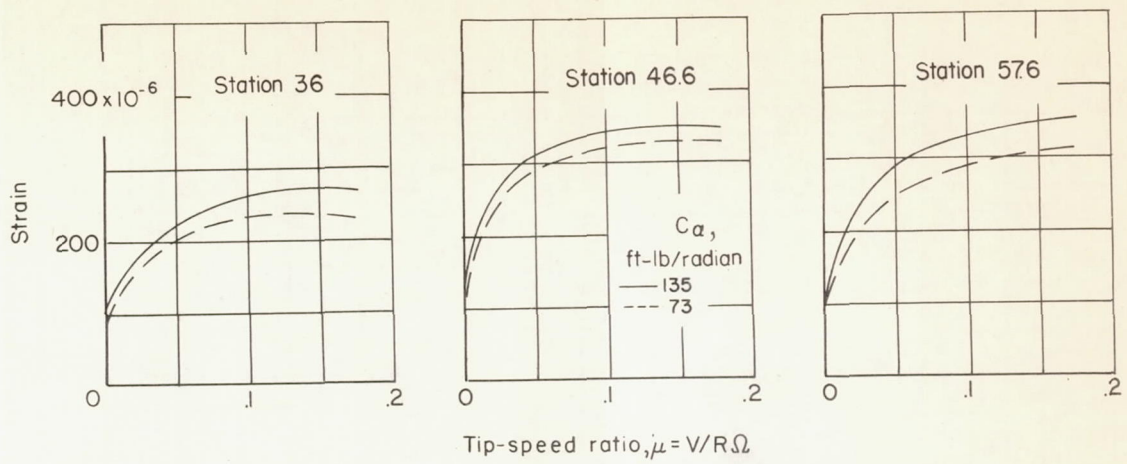

(a) Configurations 10 and 11. Outboard counterweight located at station 62.5; no concentrated weights added.

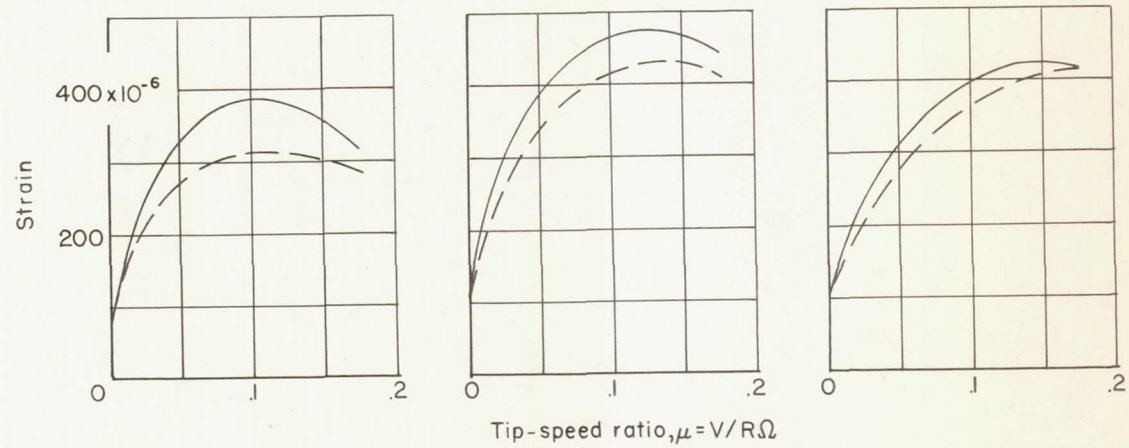

(b) Configurations 19 and 20. Outboard counterweight at station 62.5; m/M = 0.05 at station 34 at 60 percent chord.

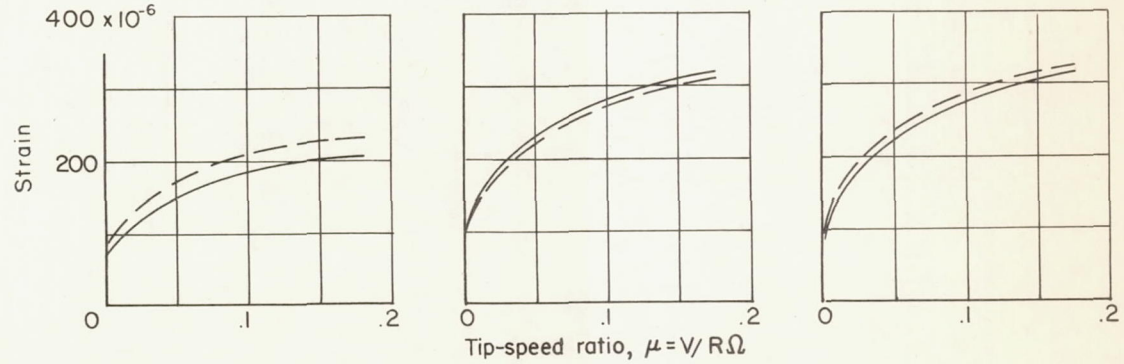

(c) Configurations 29 and 30. Outboard counterweight at station 66.5; m/M = 0.05 at station 62.5 at blade leading edge.

Figure 18.- Effect of blade-pitch-control stiffness on periodic blade bending strains.

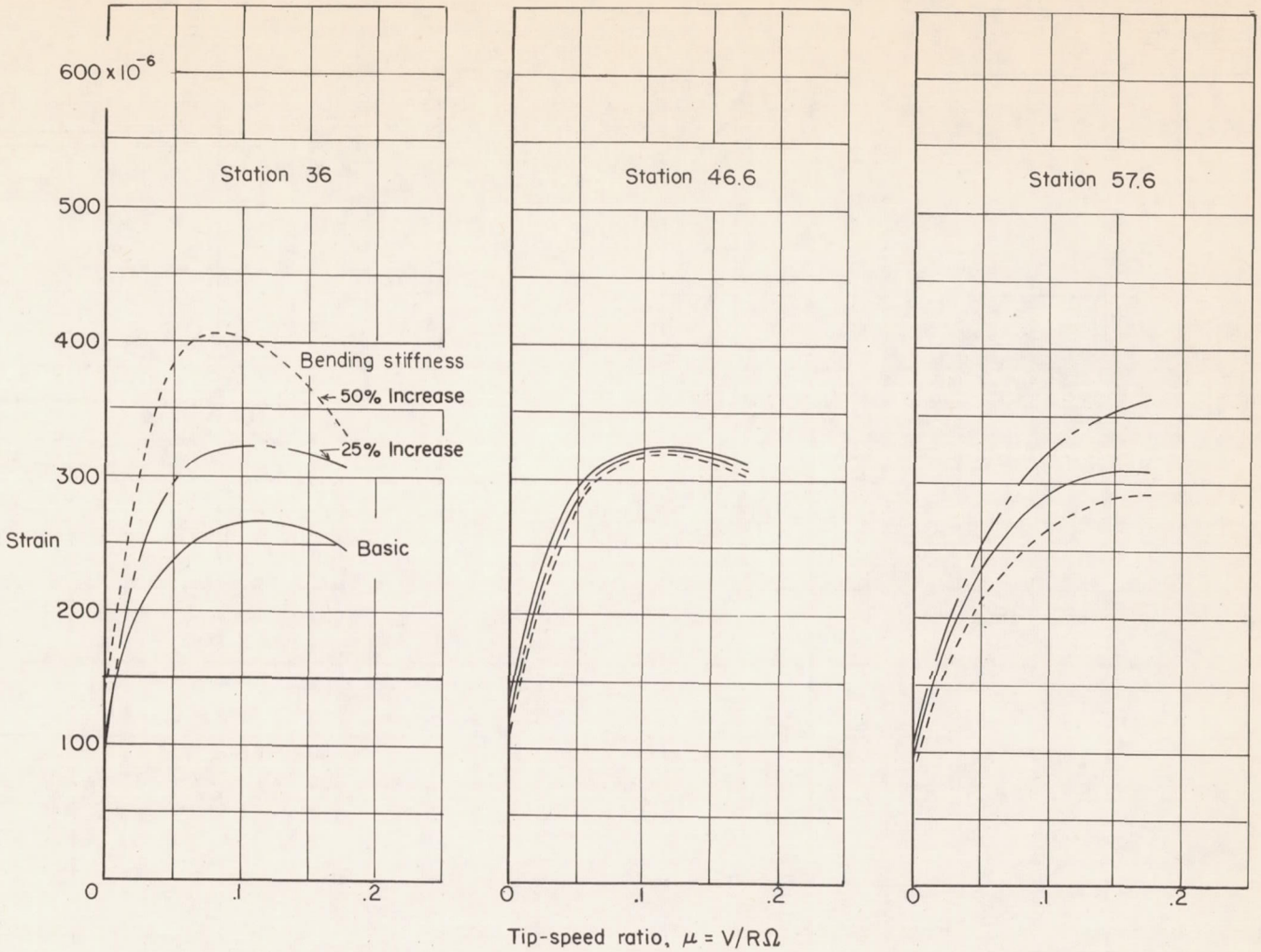

Figure 19.- Effect of increasing blade bending stiffness between stations 43 and 64 on periodic blade bending strains. Configurations 2, 52, and 53.

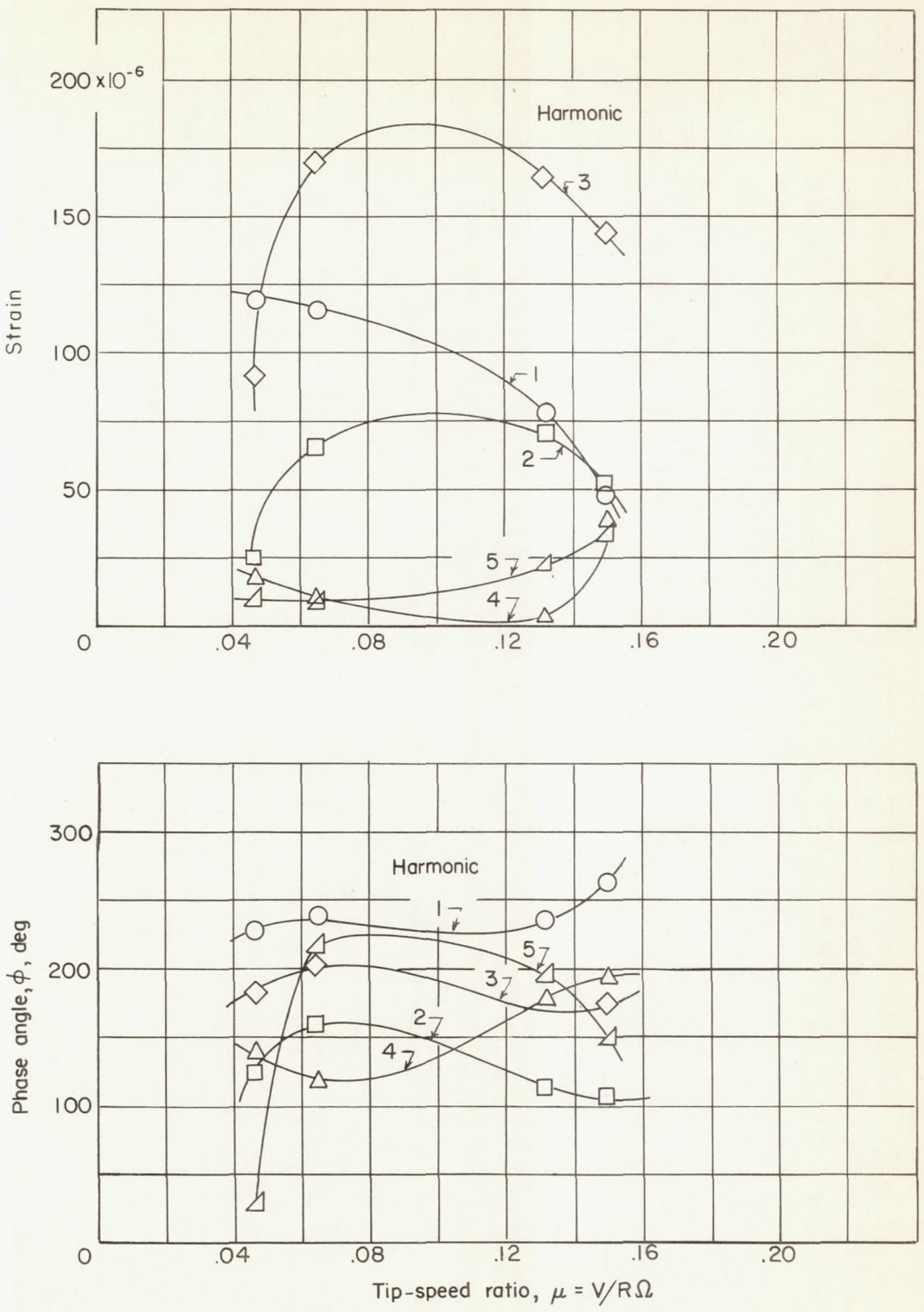

Figure 20.- Typical effect of tip-speed ratio on amplitudes and phase angles of the first five harmonic components of periodic blade bending strains. (Basic configuration, configuration 2.)

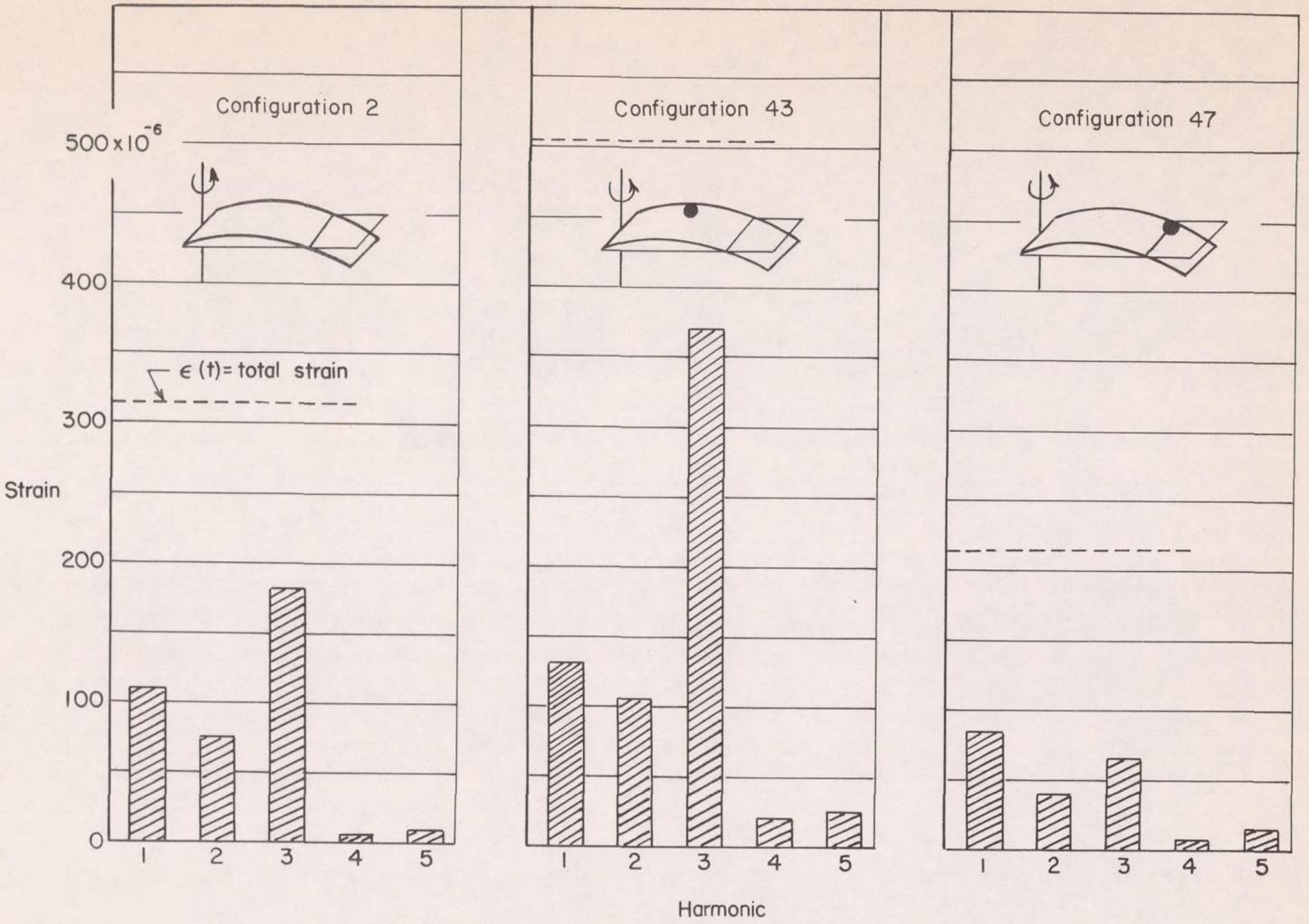

Figure 21.- Effect of the addition of concentrated weights at different radial locations on the amplitudes of the first five harmonic components of the periodic blade bending strains. $\mu = 0.08$.